Inorganic Chemistry

Article

pubs.acs.org/IC

Synthesis and Structural Characterization of a Family of Modified Hafnium *tert*-Butoxide for Use as Precursors to Hafnia Nanoparticles

Timothy J. Boyle,*[,†] Leigh Anna M. Steele,[†] Patrick D. Burton,[‡] Sarah M. Hoppe,[†] Chelsea Lockhart,[†] and Mark A. Rodriguez[†]

[†]Sandia National Laboratories, Advanced Materials Laboratory, 1001 University Boulevard SE, Albuquerque, New Mexico 87106, United States

[‡]Department of Chemical and Nuclear Engineering, Center for Micro-Engineered Materials, University of New Mexico, Albuquerque, New Mexico 87131, United States

ABSTRACT: A series of modified, hafnium *tert*-butoxide ($[Hf(OBu^t)_4]$) compounds (**1**−**26**) were crystallographically characterized, and representative species were then used to produce HfO_2 nanoparticles. This systematically varied family of $[Hf(OR)_4]$ compounds was developed from the reaction of $[Hf(OBu^t)_4]$ with a series of (i) Lewis basic *solvents*, tetrahydrofuran, pyridine, or 1-methylimidazole; (ii) simple *phenols*, $HOC_6H_4(R)$-2 or $HOC_6H_3(R)_2$-2,6 where R = CH_3, $CH(CH_3)_2$, or $C(CH_3)_3$; and (iii) *complex polydentate alcohols*, tetrahydrofuran methanol (H-OTHF), pyridinecarbinol (H-OPy), and tris(hydroxymethyl-ethane) (THME-H_3). The *solvent*-modified products were crystallographically characterized as $[Hf(OBu^t)_4(solv)_n]$ (**1**−**3**). The *phenoxide* (OAr)-exchanged $[Hf(OBu^t)_4]$ products isolated from toluene were characterized as dimeric $[Hf(OAr)_n(OBu^t)_{4-n}]_2$ (**4** and **5**) or $[Hf(\mu\text{-}OH)(OAr)_3(HOBu^t)]_2$ (**6** and **7**) for the less sterically demanding OAr ligands and $[Hf(OAr)_n(OBu^t)_{4-n}(HOBu^t)]$ (**8** and **9**) monomers for the larger OAr ligands. When Lewis basic solvents were employed, solvated monomers of varied OAr substitutions were observed as $[Hf(OAr)_n(OBu^t)_{4-n}(solv)_x]$, where solv = THF (**10**, **11**, and **13**−**15**) and py (**16** and **19**−**21**). The nuclearities of the remaining *complex polydentate alcohol* derivatives ranged from monomers (**24**, OPy) to dimers (**22**, OTHF; **23**, OPy) to tetramers (**25** and **26**, THME). On the basis of their nuclearities, select members of this family of $[Hf(OR)_4]$ compounds (monomer, $[Hf(OBu^t)_4]$, **8**; dimer, **19a**, **22**; tetramer, **25**) were used to determine the validity of using $[Hf(OR)_4]$ precursors for the production of hafnia (HfO_2) nanoparticles under solvothermal (oleylamine/oleic acid) conditions. After a 650 °C thermal treatment, the resulting powder X-ray diffraction pattern for each powder was found to be consistent with HfO_2 (PDF 00-040-1173), and after a 1000 °C treatment, larger particles of HfO_2 (PDF 00-043-1017) were reported. Transmission electron microscopy images confirmed that nanomaterials had formed. Because identical processing conditions had been employed for each HfO_2 nanomaterial, the morphological variations observed in this study may be attributed to the individual precursors ("precursor structure affect").

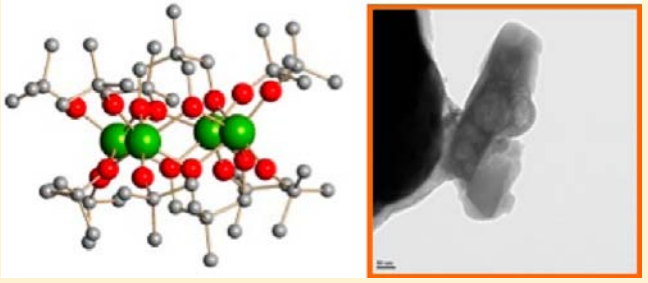

INTRODUCTION

Oxide materials of the group 4 metals have found widespread use in a variety of daily applications, such as food coloring agents, transistors, photocatalysts, dental implants, sunscreens, paints, thermal barrier coatings, and many more. While a number of precursors have been used to generate these ceramic oxides, metal alkoxides ($[M(OR)_x]$) have found favor because of the ease with which their physical properties (i.e., high solubility, low thermal decomposition, low C retention, etc.) can be tuned simply by altering the ligand set. Because $[M(OR)_x]$ precursor structures have been found to play a role in determining the final materials' properties,[1−11] understanding their coordination behavior is of interest. Thus, a great deal of effort has focused on structurally identifying $[Ti(OR)_4]$ and $[Zr(OR)_4]$ precursors;[12] however, significantly less effort has been proffered concerning the identification of $[Hf(OR)_4]$.[12−16] This is surprising because hafnia (HfO_2)-based materials are employed in a number of important applications, including neutron absorbers ("getters") for nuclear control rods, electroceramic devices such as nonvolatile computer memories, high dielectric constant (k) barrier materials for metal oxide semiconductor field effect transistors, heat mirrors, and sensors to mention a few.

We are interested in exploiting the high-k properties of HfO_2 nanowires for semiconductor applications; however, only a handful of synthesis efforts concerning HfO_2 nanomaterials have been reported.[17−22] Of the different methods available, solution routes are preferred because of the simple experimental setup and their amenability to large-scale production. The reported solution routes to HfO_2[20−22] were found to employ in situ generated $[Hf(OR)_4]$; therefore, it was reasoned that by starting with well-characterized $[Hf(OR)_4]$ compounds, higher purity HfO_2 with more control over the final morphologies would be available. Because of the impact that the

Received: December 5, 2011
Published: November 6, 2012

   dx.doi.org/10.1021/ic300622h | *Inorg. Chem.* 2012, 51, 12075−12092

arrangement of $[M(OR)_4]$ has on the final properties of nanomaterials,[1−11] coupled with the void in structurally characterized $[Hf(OR)_4]$,[13−16,23] it was of interest to generate a variety of $[Hf(OR)_4]$ prior to initiating a study on their utility for the production of tailored HfO_2 nanomaterials.

The commercially available monomeric[11] precursor hafnium *tert*-butoxide ($[Hf(OBu^t)_4]$) was selected as the starting synthon because it is a soluble oil, which was thought to facilitate the substitution reactions shown in eq 1. The ligands employed included (a) simple *phenols*, (HOAr) = $HOC_6H_4(R)$-2 or $HOC_6H_3(R)_2$-2,6 where R = CH_3, $CH(CH_3)_2$, $C(CH_3)_3$; (b) *complex polydentate alcohols*, tetrahydrofuran methanol (H-OTHF or $(OC_4H_7)^{cy}(CH_2OH)$-2), pyridinecarbinol (H-OPy or $(NC_5H_4)^{cy}$-(CH_2OH)-2) where "cy" denotes cyclic, and tris(hydroxymethyl-ethane) (THME-H_3 or $(HOCH_2)_3CCH_3$) in a series of Lewis basic *solvents* of (i) tetrahydrofuran (THF), (ii) pyridine (py), or (iii) 1-methylimidazole (MeIm). Schematics of the ligands investigated in this effort are shown in Figure 1a−j. Table 1 lists the products isolated, and the full list of compounds follows.

$$[Hf(OBu^t)_4] + n\text{HOR} \xrightarrow{\text{solv}} [Hf(OBu^t)_{4-n}(OR)_n] + n\text{HOBu}^t \quad (1)$$

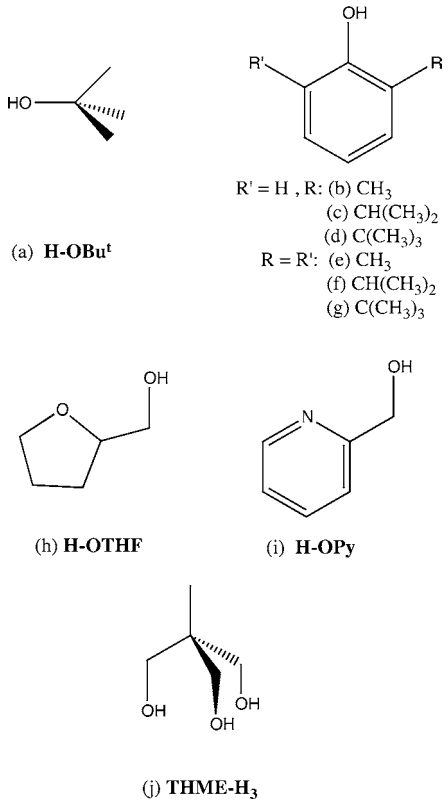

Figure 1. Schematic representation of the various ligands employed in this study: (a) $HOC(CH_3)_3$ ($HOBu^t$), $HOC_6H_3(R)$-2,(R′)-6 where R′ = H and R = (b) CH_3, (c) $CH(CH_3)_2$, and (d) $C(CH_3)_3$, $HOC_6H_3(R)$-2,(R′)-6 where R′ = R = (e) CH_3, (f) $CH(CH_3)_2$, (g) $C(CH_3)_3$, (h) $(OC_4H_7)^{cy}(CH_2OH)$-2 (H-OTHF), (i) $(NC_5H_4)^{cy}(CH_2OH)$-2 (H-OPy), and (j) $(HOCH_2)_3CCH_3$ (THME-H_3).

The *solvent* derivatives (Table 1) of $[Hf(OBu^t)_4]$ were characterized as $[Hf(OBu^t)_4(solv)_n]$ [n = 1: THF (**1**); n = 2: py (**2**), MeIm (**3**)]. The *phenoxide*-modified products were also identified by single-crystal X-ray diffraction as

Table 1. List of Products from Equation 1[a]

	SOLV			
OR	*tol*	*THF*	*py*	*MeIm*
OBu^t		1	2	3
OC_6H_4R-2				
R = CH_3	4, 4a	10	16	
= $CH(CH_3)_2$	5, 5a	11	----	
= $C(CH_3)_3$	6	----	----	
OC_6H_3R-2,6				
R = CH_3	7	13	19, 19a	
= $CH(CH_3)_2$	8	14	20	
= $C(CH_3)_3$	9	15	21	
OTHF *($(OC_4H_7)^{cy}(CH_2O)$-2)*		22		
OPy *($(NC_5H_4)^{cy}(CH_2O)$-2)*	23		24	
THME *($(OCH_2)_3CCH_3$)*	25, 26			

[a]– = crystal not isolated. Blue = solvates of $[Hf(OBu^t)_4]$. Orange = phenoxide (i) tol, (ii) THF, and (iii) py. Green = polydentate.

$[Hf(\mu\text{-}OC_6H_4(CH_3)\text{-}2)(OC_6H_4(CH_3)\text{-}2)_3(HOBu^t)]_2$ (**4**), $[Hf_2(\mu_3\text{-}O)(\mu\text{-}OH)(\mu\text{-}OC_6H_4(CH_3)\text{-}2)(OC_6H_4(CH_3)\text{-}2)_4(HOBu^t)]_2\cdot$tol (**4a**), $[Hf(\mu\text{-}OC_6H_4(CH(CH_3)_2)\text{-}2)(OBu^t)_3]_2$ (**5**), $[H][Hf_3(\mu_3\text{-}O_2(\mu\text{-}OBu^t)_3(OC_6H_4(CH(CH_3)_2)\text{-}2)_6]$ (**5a**), $[Hf(\mu\text{-}OH)(OC_6H_4(C(CH_3)_3)\text{-}2)_3(HOBu^t)]_2\cdot$2tol (**6**), $[Hf(\mu\text{-}OH)(OC_6H_3(CH_3)_2\text{-}2,6)_3(HOBu^t)]_2$ (**7**), $[Hf(OC_6H_3(CH(CH_3)_2)_2\text{-}2,6)_4(HOBu^t)]$ (**8**), $[Hf(OC_6H_3(C(CH_3)_3)_2\text{-}2,6)(OBu^t)_3(HOBu^t)]$ (**9**), $[Hf(OC_6H_4(CH_3)\text{-}2)_4(THF)_2]$ (**10**), $[Hf(OC_6H_4(CH(CH_3)_2)\text{-}2)_2(OBu^t)_2(THF)_2]$ (**11**), $[Hf(OC_6H_3(CH_3)_2\text{-}2,6)_4(THF)]$ (**13**), $[Hf(OC_6H_3(CH(CH_3)_2)_2\text{-}2,6)_3(OBu^t)(THF)]$ (**14**), $[Hf(OC_6H_3(C(CH_3)_3)_2\text{-}2,6)(OBu^t)_3(THF)]$ (**15**), $[Hf(OC_6H_4(CH_3)\text{-}2)_4(py)_2]\cdot$py (**16**), $[Hf(OC_6H_3(CH_3)_2\text{-}2,6)_4(py)_2]$ (**19**), $[Hf(\mu\text{-}OH)(OC_6H_3(CH_3)_2\text{-}2,6)_3(py)]_2\cdot$3py (**19a**), $[Hf(OC_6H_3(CH(CH_3)_2)_2\text{-}2,6)_3(OBu^t)(py)]$ (**20**), and $[Hf(OC_6H_3(C(CH_3)_3)_2\text{-}2,6)(OBu^t)_3(py)]$ (**21**). The remaining *complex polydentate alcohol* derivatives were solved as $[Hf(\mu_c\text{-OTHF})(OBu^t)_3]_2$ (**22**), $[Hf_2(OBu^t)_4(\mu_c\text{-OPy})_3(OPy)]$ (**23**), $[(OPy)^c{}_2Hf(OBu^t)_2]$ (**24**), and $[(\mu\text{-THME})(\mu\text{-OR})Hf_2(OR)_4]_2$ [OR = OBu^t (**25**) and ONep ($OCH_2C(CH_3)_3$ (**26**) where "*c*" denotes chelation]. *Note:* Crystals could not be isolated in our hands for compounds **12** $[OC_6H_4(C(CH_3)_3)\text{-}2/THF]$, **17** $[OC_6H_4(CH(CH_3)_2)\text{-}2/py]$, and **18** $[OC_6H_4(C(CH_3)_3)\text{-}2/py]$. The synthesis and characterization of the precursor compounds **1**−**26** are discussed in detail.

With this novel set of well-characterized precursors (**1**−**26**) now available, select members having varied nuclearity (monomer, $[Hf(OBu^t)_4]$, **8**; dimer, **19a**, **22**; tetramer, **25**) were processed under solvothermal (SOLVO) conditions to generate the first alkoxide precursor solution route to HfO_2 nanoparticles. The compounds were chosen based on their nuclearities to demonstrate their utility as HfO_2 precursors and initiate a study on the precursor structure affect (PSA).[4,9,10] Details of the synthesis, crystal structures, and preliminary investigation into the nanomaterials generated from this novel family of $[Hf(OR)_4]$ compounds will be discussed.

■ EXPERIMENTAL SECTION

All reactions were performed under a dry, inert atmosphere using standard Schlenk-line and glovebox techniques. The following chemicals were used as received from Aldrich: $[Hf(OBu^t)_4]$, HOAr = $HOC_6H_4(R)$-2 and $HOC_6H_3(R)_2$-2,6 (where R = CH_3, $CH(CH_3)_2$, $C(CH_3)_3$), $(OC_4H_7)^{cy}(CH_2OH)$-2 (H-OTHF), $(NC_5H_4)^{cy}(CH_2OH)$-2 (H-OPy), $(HOCH_2)_3CCH_3$ (THME-H_3). All anhydrous solvents

dx.doi.org/10.1021/ic300622h | *Inorg. Chem.* 2012, 51, 12075−12092

(tol, THF, py, and MeIm) were used as received (Aldrich) in Sure/Seal bottles and handled under an inert atmosphere.

Fourier transform infrared (FTIR) spectral data were obtained on a Nicolet 6700 FTIR spectrometer using KBr pellets pressed under an argon atmosphere and handled under an atmosphere of flowing nitrogen. Elemental analyses were performed on a Perkin-Elmer 2400 CHN-S/O elemental analyzer. All NMR samples were prepared by dissolving crystalline material in the appropriate deuterated solvent followed by flame sealing under vacuum. Spectra were collected on a Bruker Avance 500 NMR spectrometer, using a 5 mm inverse probe, under standard experimental conditions: ^{1}H analyses were performed with a 4-s recycle delay at 16 scans; spectra were referenced to the residual proton peak of chloroform-*d* ($CDCl_3$) at 7.24 ppm, toluene-d_8 (tol-d_8) peak at 2.09 ppm, tetrahydrofuran-d_8 (THF-d_8) at 1.79 ppm, or pyridine-d_5 (py-d_5) at 8.75 ppm.

General Synthesis of [Hf(OBu^t)$_4$(solv)$_x$]. A sample of [Hf(OBu^t)$_4$] (1.0 g, 2.1 mmol) was added to a vial containing the desired solvent (~3 mL). The resultant precipitate was heated until the reaction turned clear. After cooling to room temperature, the reaction mixture was allowed to set uncovered until crystals formed.

*[Hf(OBu^t)$_4$(THF)] (**1**).* Solvent used: THF. Yield: 0.68 g (59%). FTIR (KBr, cm^{-1}): 2970(s), 2916(m,sh), 2888(m,sh), 2851(m,sh), 1459(m), 1384(m), 1358(s), 1243(m,sh), 1228(m,sh), 1191(s), 1018(s), 991(s), 903(m), 781(br,m), 701(w), 669(w), 568(m), 527(m), 493(m), 475(m). ^{1}H NMR (500.1 MHz, THF-d_8): δ 1.63 (OC(CH_3)$_3$). Elem anal. Calcd for $C_{20}H_{44}HfO_5$ (MW = 543.05): C, 44.23; H, 8.17. Found: C, 37.40; H, 7.37.

*[Hf(OBu^t)$_4$(py)$_2$] (**2**).* Solvent used: py. Yield: 1.3 g (97%). FTIR (KBr, cm^{-1}): 2970(s), 2916(m,sh), 2888(m,sh), 2851(m,sh), 1460(m), 1425(m), 1385(m), 1458(m), 1359(s), 1243(m,sh), 1214(m,sh), 1201(s), 1025(s,sh), 1021(s), 995(s), 908(m), 901(m), 850(w), 682(w), 667(w), 568(m), 530(m), 492(m), 476(m). ^{1}H NMR (500.1 MHz, py-d_5): δ 1.40 (OC(CH_3)$_3$). Elem anal. Calcd for $C_{26}H_{46}HfN_2O_4$ (MW = 629.14): C, 49.64; H, 7.37; N, 4.45. Found: C, 48.15; H, 7.57; N, 4.29.

*[Hf(OBu^t)$_4$(MeIm)$_2$] (**3**).* Solvent used: tol with MeIm (~5 drops). Washed repeatedly with hexanes and toluene. Yield: 1.2 g (89%). FTIR (KBr, cm^{-1}): 2963(s), 2910(m,sh), 2897(m,sh), 2866(m,sh), 2842(m,sh), 1560(m), 1530(m), 1473(m), 1457(m), 1422(m), 1374(m), 1348(m), 1199(s), 1108(m), 1085(m), 1019(s), 936(m), 830(w), 825(w), 739(m), 661(m), 617(w), 500(m), 478(m). Elem anal. Calcd for $C_{24}H_{48}HfN_4O_4$ (MW = 635.15): C, 45.38; H, 7.62; N, 8.82. Found: C, 41.27; H, 6.84; N, 7.29.

General Synthesis of HOAr-Modified [Hf(OBu^t)$_4$]. The desired ligand was added to a vial containing [Hf(OBu^t)$_4$] fully dissolved in the solvent of choice. In some instances (noted below), the reaction mixture was placed directly into a freezer at −40 °C. Otherwise, the reaction mixture was stirred for 24 h and then allowed to sit with the cap loose until crystals formed. Yields were based on the first crystalline batch. Analytical data were collected on dried crystalline material.

*[Hf(μ-OC$_6$H$_4$(CH$_3$)-2)(OC$_6$H$_4$(CH$_3$)-2)$_3$(HOBu^t)]$_2$ (**4**).* [Hf(OBu^t)$_4$] (0.50 g, 1.1 mmol) and H-OC$_6$H$_4$(CH$_3$)-2 (0.46 g, 4.3 mmol) in ~5 mL of tol. Yield: 39% (0.28 g). FTIR (KBr, cm^{-1}): 2969(s), 2960(w), 1813(w), 1672(m, sh), 1487(s), 1360(m), 1292(m,sh), 1263(s), 1191(s), 1113(m), 1043(s), 899(w), 848(m), 793(w,sh), 757(s), 700(s), 633(s), 598(s), 538(m), 479(s). ^{1}H NMR (500.1 MHz, $CDCl_3$): δ 7.10 (4.0H, d, OC$_6$$H_4$(CH$_3$)-2), J_{H-H} = 6.8 Hz), 6.93 (3.9H, s, br), OC$_6$$H_4$(CH$_3$)-2)), 6.82 (4.1H, t, OC$_6$$H_4$(CH(CH$_3$)$_2$-2), J_{H-H} = 7.1 Hz), 6.73 (3.7H, s(br), OC$_6$$H_4$(CH$_3$)-2)), 2.04 (12.4H, s(br), OC$_6$H$_4$(CH_3)-2), 1.29 (10.4H, s, OC(CH_3)$_3$)). Elem anal. Calcd for $C_{64}H_{76}Hf_2O_{10}$ (MW = 1362.26): C, 56.43; H, 5.62. Found: C, 54.24; H, 5.49.

*[Hf(μ-OC$_6$H$_4$(CH(CH$_3$)$_2$)-2)(OBu^t)$_3$]$_2$ (**5**).* [Hf(OBu^t)$_4$] (0.50 g, 1.1 mmol) and H-OC$_6$H$_4$(CH(CH$_3$)$_2$)-2 (0.14 g, 1.1 mmol) in ~1.5 mL of tol. Yield: 37% (0.21 g, crystals isolated at −40 °C). FTIR (KBr, cm^{-1}): 3065(w), 3021(w), 2967(s), 2928(s) 2908(s,sh), 2868(s,sh), 1655(w), 1593(m), 1577(m), 1572(m), 1560(m), 1508(m), 1485(s), 1445(s), 1382(m,sh), 1361(s,br), 1291(s), 1262(s), 1232(m), 1197(s), 1146(m), 1086(s), 1033(s), 902(m), 872(m), 789(m), 755(s), 483(s,sh), 472(s), 465(s,sh). ^{1}H NMR (500.1 MHz, $CDCl_3$): δ 7.23 (0.8H, d, OC$_6$$H_4$(CH(CH$_3$)$_2$)-2), J_{H-H} = 7.8 Hz), 7.01 (1.2H, d, OC$_6$$H_4$(CH(CH$_3$)$_2$-2), J_{H-H} = 7.3 Hz), 6.91 (1.1H, t, OC$_6$$H_4$(CH(CH$_3$)$_2$-2), J_{H-H} = 6.9 Hz), 6.73 (0.9H, t, OC$_6$$H_4$(CH(CH$_3$)$_2$)-2), J_{H-H} = 7.3 Hz), 3.32 (0.9, sept, OC$_6$H$_4$(CH(CH$_3$)$_2$-2), J_{H-H} = 6.7 Hz), 1.17 (5.0H, d, OC$_6$H$_4$(CH(CH_3)$_2$-2), J_{H-H} = 6.7 Hz), 0.90 (27H, s, OC(CH_3)$_3$). Elem anal. Calcd for $C_{42}H_{76}Hf_2O_8$ (MW = 1066.01): C, 47.32; H, 7.19. Found: C, 45.57; H, 7.18.

*[Hf(μ-OH)(OC$_6$H$_4$(C(CH$_3$)$_3$)-2)$_3$(HOBu^t)]$_2$·2tol (**6**).* [Hf(OBu^t)$_4$] (0.47 g, 1.0 mmol) and H-OC$_6$H$_4$(C(CH$_3$)$_3$)-2 (0.60 g, 4.0 mmol) in ~3 mL of tol. Yield: 67% (0.54 g). FTIR (KBr, cm^{-1}): 3853(w), 3095(w), 3077(w), 3047(w), 3009(m), 2969(s), 2361(w), 1917(w), 1879(w), 1594(m), 1569(m), 1485(s), 1438(s), 1386(m), 1362(s), 1294(s), 1270(s), 1233(s), 1195(s), 1130(m), 1090(m), 1055(m), 1030(s), 998(s), 875(s), 861(s), 829(m), 788(m), 756(s), 742(s), 693(m), 616(m), 569(m), 542(m), 525(m), 487(m), 441(m). ^{1}H NMR (500.1 MHz, tol-d_8): δ 7.29 (6.0H, d, OC$_6$$H_4$(C(CH$_3$)$_3$-2), J_{H-H} = 7.6 Hz), 6.79 (5.8H, t, OC$_6$$H_4$(C(CH$_3$)$_3$-2), J_{H-H} = 7.9 Hz), 1.53 (24.1H, s, OC$_6$H$_4$(C(CH_3)$_3$-2)), 1.23 (14.1H, s, OC(CH_3)$_3$). Elem anal. Calcd for $C_{82}H_{114}Hf_2O_{10}$ (MW = 1616.76): C, 60.92; H, 7.11. Found: C, 58.71; H, 6.89.

*[Hf(μ-OH)(OC$_6$H$_3$(CH$_3$)$_2$-2,6)$_3$(HOBu^t)]$_2$ (**7**).* [Hf(OBu^t)$_4$] (0.50 g, 1.1 mmol) and H-OC$_6$H$_3$(CH$_3$)$_2$-2,6 (0.52 g, 4.3 mmol) in ~10 mL of tol. Yield: 72% (0.48 g). FTIR (KBr, cm^{-1}): 3422(s,br), 3068(w), 3039(w), 3019(w), 3010(w), 2962(s), 2924(s), 2855(s), 2733(w), 1592(m), 1561(w), 1508(w), 1473(s), 1437(s,sh), 1427(s), 1401(w), 1372(w), 1276(s), 1231(s), 1170(w), 1161(w), 1092(s), 1044(m), 1033(m), 983(w), 888(s), 863(m), 801(m), 760(s), 735(m), 719(m), 550(m), 489(w), 467(m), 155(m), 446(m). ^{1}H NMR (500.1 MHz, tol-d_8): δ 6.88 (2.4H, d, OC$_6$$H_3$(CH$_3$)$_2$-2,6, J_{H-H} = 7.3 Hz), 6.69 (1.4H, t OC$_6$$H_3$(CH$_3$)$_3$-2), 2.20 (6.0H, s(br), OC$_6$H$_4$(CH_3)$_2$-2,6), 0.98 (2.6H, s, OC(CH_3)$_3$). Elem anal. Calcd for $C_{56}H_{76}Hf_2O_{10}$ (MW = 1266.18): C, 53.12; H, 6.05. Found: C, 58.71; H, 6.89.

*[Hf(OC$_6$H$_3$(CH(CH$_3$)$_2$)$_2$-2,6)$_4$(HOBu^t)] (**8**).* [Hf(OBu^t)$_4$] (0.47 g, 1.0 mmol) and H-OC$_6$H$_3$(CH(CH$_3$)$_2$)$_2$-2,6 (0.71 g, 4.0 mmol) in ~3 mL of tol. Yield: 60% (0.57 g). FTIR (KBr, cm^{-1}): 3905(w), 3886(w), 3855(w), 3822(w), 3808(w), 3753(w), 3745(w), 3713(w), 3676(w), 3657(w), 3630(w), 3566(s), 3175(w), 3062(m), 3024(m), 2963(s), 2868(s), 2586(m), 2302(w), 1902(w), 1845(w), 1794(w), 1697(w), 1641(w), 1588(m), 1435(s), 1382(s), 1361(s), 1325(s), 1259(s), 1200(s), 1159(s), 1112(s), 1095(s), 1041(s), 1016(s), 951(w), 936(m), 892(s), 870(s), 822(m), 805(m), 793(s), 749(s), 704(s), 623(w), 587(w), 551(w), 536(w), 473(m), 445(w), 422(m), 405(m). ^{1}H NMR (500.1 MHz, tol-d_8): δ 7.03 (2.0H, d, OC$_6$$H_3$(CH(CH$_3$)$_2$-2,6), J_{H-H} = 7.6 Hz), 6.88 (1.0H, t, OC$_6$$H_3$(CH(CH$_3$)$_2$-2,6), J_{H-H} = 7.6 Hz), 3.38 (1.6H, s(br), OC$_6$H$_3$(CH(CH$_3$)$_2$-2,6), 1.33 (2.2H, s, OC(CH_3)$_3$), 1.12 (11.4H, s(br), OC$_6$H$_3$(CH(CH$_3$)$_2$-2,6)). Elem anal. Calcd for $C_{52}H_{78}HfO_5$ (MW = 961.66): C, 64.95; H, 8.18. Found: C, 62.25; H, 7.62

*[Hf(OC$_6$H$_3$(C(CH$_3$)$_3$)$_2$-2,6)(OBu^t)$_3$(HOBu^t)] (**9**).* [Hf(OBu^t)$_4$] (0.41 g, 0.87 mmol) and H-OC$_6$H$_3$(C(CH$_3$)$_3$)-2,6 (0.18 g, 0.87 mmol) in ~3 mL of tol. Yield: 44% (0.26 g, crystals isolated at −40 °C). FTIR (KBr, cm^{-1}): 3062(w), 2966(s), 2926(s), 2870(m), 1420(m), 1389(m), 1360(m), 1262(m), 1231(w), 1189(m), 1094(s), 1050(s), 1016(s), 889(m), 844(w), 797(s), 746(s), 747(m), 676(w), 469(s,br). ^{1}H NMR (500.1 MHz, $CDCl_3$): δ 7.23 (2.0H, d, (OC$_6$$H_3$(C(CH$_3$)$_3$)$_2$-2,6), J_{H-H} = 7.7 Hz), 6.78 (0.8H, s(br), (OC$_6$$H_3$(C(CH$_3$)$_3$)$_2$-2,6)), 1.50 (17H, s, O(C(CH_3)$_3$)$_2$-2,6), 1.33 (27H, s, OC(CH_3)$_3$). Elem anal. Calcd for $C_{30}H_{58}HfO_5$ (MW = 677.27): C, 53.20; H, 8.63. Found: C, 50.47; H, 8.11.

*[Hf(OC$_6$H$_4$(CH$_3$)-2)$_4$(THF)$_2$] (**10**).* [Hf(OBu^t)$_4$] (0.50 g, 1.1 mmol) and H-OC$_6$H$_4$(CH$_3$)-2 (0.46 g, 4.3 mmol) in ~3 mL of THF. Yield: 79% (0.63 g). FTIR (KBr, cm^{-1}): 3066(m), 3016(m), 2982(m), 2966(m), 2926(m), 2882(m), 2871(m), 1596(s), 1578(m), 1546(w), 1487(s), 1460(m), 1387(w), 1280(sh,s), 1277(s), 1265(s), 1230(m), 1208(w), 1188(w), 1167(w), 1155(w), 1114(s), 1042(s), 1042(m), 984(w), 932(w), 895(s), 884(s), 858(m), 805(w), 773(sh,m), 752(s), 734(sh,m), 714(m), 630(m), 582(m), 559(w), 526(m), 463(m), 412(w). ^{1}H NMR (500.1 MHz, THF-d_8): δ 6.69 (1H, d, OC$_6$$H_4$-(CH$_3$)-2, J_{H-H} = 3.6 Hz), 6.83 (1H, t, OC$_6$$H_4$(CH$_3$)-2, J_{H-H} = 7.4 Hz),

dx.doi.org/10.1021/ic300622h | Inorg. Chem. 2012, 51, 12075−12092

6.74 (1H, d, OC6H4(CH_3)-2, J_{H-H} = 3.6 Hz), 6.53 (1H, t, OC_6H_4-(CH_3)-2, J_{H-H} = 7.3 Hz), 2.14 (3H, s, $OC_6H_4(CH_3)$-2). Elem anal. Calcd for $C_{36}H_{44}HfO_6$ (MW = 751.22): C, 57.56; H, 5.90. Found: C, 57.04; H, 6.10.

[Hf(OC$_6$H$_4$(CH(CH$_3$)$_2$)-2)$_2$(OBu^t)$_2$(THF)$_2$] ***(11)***. [Hf(OBu^t)$_4$] (0.50 g, 1.1 mmol) and H-$OC_6H_4(CH(CH_3)_2)$-2 (0.30 g, 2.1 mmol) in ~3 mL of THF. Yield: 68% (0.53 g). FTIR (KBr, cm^{-1}): 3023(m), 3066(m), 2961(s), 2926(m), 2909(m), 2867(m), 1593(m), 1574(m), 1483(s), 1444(s), 1382(m), 1361(m), 1345(m), 1285(s), 1255(br,s), 1271-(m,sh), 1193(m), 1174(m), 1147(m), 1111(w), 1085(m), 1033(m), 1012(w), 901(s), 874(s), 860(s), 841(sh,m), 753(s), 627(m), 572(m), 533(w), 497(w), 468(w), 426(w). ^{1}H NMR (500.1 MHz, $CDCl_3$): δ 7.08 (1H, d, $OC_6H_4(CH(CH_3)_2$-2), J_{H-H} = 7.0 Hz), 7.04 (1H, d, $OC_6H_4(CH(CH_3)_2$-2, J_{H-H} = 6.9 Hz), 6.60 (1H, multiplet, $OC_6H_4(CH(CH_3)_2$-2)), 6.54 (1H, multiplet, $OC_6H_4(CH_3)$-2), 3.72 (1H, multiplet, $OC_6H_4(CH(CH_3)_2$-2), 1.27 (8.5H, s, $OC(CH_3)_3$), 1.16 (6.7H, d, $OC_6H_4(CH(CH_3)_2$-2), J_{H-H} = 6.9 Hz). Elem anal. Calcd for $C_{34}H_{56}HfO_6$ (MW = 739.29): C, 55.24; H, 7.63. Found: C, 58.88; H, 6.81.

[Hf(OC$_6$H$_3$(CH$_3$)$_2$-2,6)$_4$(THF)] ***(13)***. [Hf(OBu^t)$_4$] (0.50 g, 1.1 mmol) and H-$OC_6H_3(CH_3)_2$-2,6 (0.52 g, 4.3 mmol) in ~3 mL of THF. Yield: 50% (0.39 g). FTIR (KBr, cm^{-1}): 3067(m), 3040(m), 3015(m), 2944(s), 2919(s), 2854(m), 2731(w), 1608(w), 1592(m), 1473(s), 1444(m,sh), 1428(s), 1276(s), 1230(s), 1159(w), 1092(s), 1072(w), 1043(w), 1015(w), 983(w), 889(s), 879(m,sh), 761(s), 735(s), 719(s), 699(w), 633(w), 550(m), 488(m), 460(m). ^{1}H NMR (500.1 MHz, THF-d_8): δ 6.76 (2H, d, $OC_6H_3(CH_3)_2$-2,6, J_{H-H} = 2.5 Hz), 6.45 (1H, t, $OC_6H_3(CH_3)_2$-2,6, J_{H-H} = 7.3 Hz), 2.08 (6.2H, s, OC_6H_3-$(CH_3)_2$-2,6). Elem anal. Calcd for $C_{36}H_{44}HfO_5$ (MW = 735.22): C, 58.81; H, 6.03. Found: C, 58.24; H, 6.03.

[Hf(OC$_6$H$_3$(C(CH$_3$)$_3$)$_2$-2,6)(OBu^t)$_3$(THF)] ***(15)***. [Hf(OBu^t)$_4$] (0.25 g, 0.53 mmol) and H-$OC_6H_3(C(CH_3)_3)_2$-2,6 (0.11 g, 0.53 mmol) in ~3 mL of THF. Yield: 28% (0.10 g). FTIR (KBr, cm^{-1}): 2970(s), 2940(s,sh), 2928(s,sh), 2916(s,sh), 2868(s), 2812(w), 1469(m), 1458(m), 1426(m), 1387(s), 1359(s), 1314(w), 1249(s), 1230(s), 1202(s), 1193(s), 1146(w) 1123(w), 1093(w), 1036(s,br), 1022(s,br), 1001(s), 910(s), 894(s), 844(w), 822(w), 806(w), 781(m), 767(m), 746(m), 727(m), 679(w), 670(w), 857(s), 567(s), 531(s), 521(s,sh), 493(s), 474(s), 448(s). ^{1}H NMR (500.1 MHz, THF-d_8): δ 7.03 (2.8H, d, $OC_6H_3(C(CH_3)_3)_2$-2,6), 6.46 (0.70H, d, $OC_6H_3(C(CH_3)_3)_2$-2,6), 1.42 (18.0H, s, $OC_6H_3(C(CH_3)_3)_2$-2,6), 1.27 (26.6H, σ, $OX(XH_3)_3$). Elem anal. Calcd for $C_{30}H_{56}HfO_5$ (MW = 675.25): C, 53.36; H, 8.36. Found: C, 42.13; H, 7.27.

[Hf(OC$_6$H$_4$(CH$_3$)-2)$_4$(py)$_2$]·py ***(16)***. [Hf(OBu^t)$_4$] (0.50 g, 1.1 mmol) and H-$OC_6H_4(CH_3)$-2 (0.46 g, 4.3 mmol) in ~3 mL of py. Yield: 75% (0.68 g). FTIR (KBr, cm^{-1}): 3064(m), 3013(m), 2963(m), 2944(m), 2925(m), 2855(m), 1624(m), 1594(m), 1485(s), 1446(m), 1324(m), 1280(s), 1266(s,sh), 1214(m), 1187(m), 1150(m), 1112(m), 1069(m), 1043(m), 1013(m), 982(w), 928(w), 907(m,sh), 896(m,sh), 881(m), 846(w), 805(w), 770(m), 753(m), 716(w), 700(m), 629(m), 617(m), 562(m), 466(m). ^{1}H NMR (500.1 MHz, py-d_5): δ 8.71 (C_5H_5), 7.56 (C_5H_5), 7.18 (1.3H, multiplet, $OC_6H_4(CH_3)$-2 and C_5H_5), 7.04 (1.1H, t, $OC_6H_4(CH_3)$-2, J_{H-H} = 7.4 Hz), 6.91 (1.0H, br s, $OC_6H_4(CH_3)$-2), 6.80 (1.1H, d, $OC_6H_4(CH_3)$-2, J_{H-H} = 3.6 Hz), 2.29 (3.0H, s, $OC_6H_4(CH_3)$-2). Elem anal. Calcd for $C_{43}H_{43}HfN_3O_4$ (MW = 845.27): C, 61.17; H, 5.13; N, 4.98. Found: C, 60.52; H, 5.25; N, 3.66.

[Hf(OC$_6$H$_3$(CH$_3$)$_2$-2,6)$_4$(py)$_2$] ***(19)***. [Hf(OBu^t)$_4$] (0.50 g, 1.1 mmol) and H-$OC_6H_3(CH_3)_2$-2,6 (0.52 g, 4.3 mmol) in ~3 mL of py. Yield: 60% (0.52 g). FTIR (KBr, cm^{-1}): 3060(w), 2963(s), 2927(m), 2869(s), 1474(m), 1459(m), 1438(s), 1382(m), 1363(m), 1329(m), 1262(s), 1207(s), 1151(m), 1113(s), 1096(s), 1060(m), 1044(m), 1018(s), 955(m), 936(m), 895(s), 873(s), 803(s), 795(s), 749(s), 704(m), 659(m), 591(m), 475(m,br). ^{1}H NMR (500.1 MHz, py-d_5): δ 8.57 (C_5H_5), 7.41 (C_5H_5), 7.05 (C_5H_5), 6.90 (2.0H, d, OC_6H_3-$(CH_3)_2$-2,6, J_{H-H} = 3.7 Hz), 6.63 (1.0H, t, $OC_6H_3(CH_3)_2$-2,6, J_{H-H} = 7.4 Hz), 1.90 (6.1H, s, $OC_6H_3(CH_3)_2$-2,6). Elem anal. Calcd for $C_{42}H_{46}HfN_2O_4$ (MW = 821.32): C, 61.42; H, 5.65; N, 3.41. Found: C, 63.42; H, 5.74; N, 4.67.

[Hf(OC$_6$H$_3$(CH(CH$_3$)$_2$)$_2$-2,6)$_3$(OBu^t)(py)] ***(20)***. [Hf(OBu^t)$_4$] (0.50 g, 1.1 mmol) and H-$OC_6H_3(CH(CH_3)_2)_2$-2,6 (0.57 g, 3.2 mmol) in ~3 mL of py. Yield: 83% (0.76 g). FTIR (KBr, cm^{-1}): 3060(br,w), 3029(w), 2963(s), 2925(m), 2869(m), 149(m), 1438(s), 1382(m), 1329(m), 1262(s), 1207(s,br), 1151(m,br), 1115(s), 1096(s), 1060(m), 1044(m), 1018(m), 955(w), 935(w), 895(s), 873(s), 801(s), 795(s), 749(s), 704(m), 669(m), 591(m), 475(br,m). ^{1}H NMR (500.1 MHz, py-d_5): δ 8.74 (C_5H_5), 7.58 (C_5H_5), 7.21 (C_5H_5), 6.90 (6.1H, d, $OC_6H_3(CH(CH_3)_2)_2$-2,6, J_{H-H} = 3.7 Hz), 6.63 (3.1H, t, OC_6H_3(CH-$(CH_3)_2)_2$-2,6, J_{H-H} = 7.4 Hz), 3.76 (6.0H, sept, $OC_6H_3(CH(CH_3)_2)_2$-2,6, J_{H-H} = 6.8 Hz), 1.39 (9.5H, s, $OC(CH_3)_3$), 1.16 (33.1H, d, $OC_6H_3(CH(CH_3)_2)_2$-2,6, J_{H-H} = 3.3 Hz). Elem anal Calcd for $C_{45}H_{65}HfNO_4$ (MW = 862.50): C, 62.67; H, 7.60; N, 1.62. Found: C, 61.92; H, 7.42; N, 2.49.

[Hf(OC$_6$H$_3$(C(CH$_3$)$_3$)$_2$-2,6)(OBu^t)$_3$(py)] ***(21)***. [Hf(OBu^t)$_4$] (0.25 g, 0.53 mmol) and H-$OC_6H_3(C(CH_3)_3)_2$-2,6 (0.11 g, 0.53 mmol) in ~3 mL of py. Yield: 67% (0.24 g). FTIR (KBr, cm^{-1}): 3016(w), 2964(s), 2923(m), 2958(m), 1477(s), 1468(s),1456(m), 1426(s), 1374(w,br). 1278(s,br), 1266(s), 1230(s), 1092(s), 1031(m,br), 982(w), 957(w), 890(s), 864(m), 802(m,br), 763(s), 734(m), 721(m), 706(w), 563(w), 551(w,br), 475(w), 463(w), 420(w). ^{1}H NMR (500.1 MHz, py-d_5): δ 8.72 (C_5H_5), 7.57 (C_5H_5), 7.43 (2.0H, d, $OC_6H_3(C(CH_3)_3)_2$-2,6), 7.22 (C_5H_5), 6.90 (0.8H, t, $OC_6H_3(C(CH_3)_3)_2$-2,6), 1.61 (18.0H, σ, OX-$(XH_3)_3$), 1.36 (32.0H, s, $OC_6H_3(C(CH_3)_3)_2$-2,6). Elem anal. Calcd for $C_{31}H_{53}HfNO_4$ (MW = 682.25): C, 54.57; H, 7.83; N, 2.05. Found: C, 53.01; H, 7.78; N, 1.93.

[Hf(μ_c-OTHF)(OBu^t)$_3$]$_2$ ***(22)***. [Hf(OBu^t)$_4$] (1.0 g, 2.1 mmol) and H-OTHF (0.22 g, 2.1 mmol) in ~1.5 mL of THF. Yield: 52% (0.55 g). FTIR (KBr, cm^{-1}): 2966(s), 2918(m,sh), 2888(m,sh), 2836(m,sh), 2760(w), 2685(w), 1465(m), 1458(m), 1380(m), 1355(s), 1205-(m,sh), 1205(m,sh), 1197(s), 1020(m,sh), 1010(s), 927(m), 815(m), 780(m), 756(m), 522(m), 480(m). NMR (500.1 MHz, $CDCl_3$): δ 4.58−4.27 (1.4H, multiplet, $OC_4H_7(CH_2O)$), 4.16−3.71 (5.5H, multiplet, $OC_4H_7(CH_2O)$), 1.94 (4.2H, s(br), $OC_4H_7(CH_2O)$), 1.25 (13.5H, s, $OC(CH_3)_3$), 1.16 (13.5H, s, $OC(CH_3)_3$). Elem anal. Calcd for $C_{34}H_{72}Hf_2O_{10}$ (MW = 997.91): C, 40.92; H, 7.27. Found: C, 41.08; H, 7.32.

[(OPy)^c$_2$Hf(OBu^t)$_2$] ***(24)***. [Hf(OBu^t)$_4$] (3.0 g, 6.3 mmol) and H-OPy (1.4 g, 13 mmol) heated in ~3 mL of tol. Yield: 56% (1.9 g). ^{1}H NMR (500.1 MHz, tol-d_8): δ 8.71 (1H, d, $NC_5H_5(CH_2O)$, J_{H-H} = 5.3 Hz), 6.81 (1.1H, t, $NC_5H_5(CH_2O)$, J_{H-H} = 7.9 Hz), 6.51 (1.2H, t, $NC_5H_5(CH_2O)$, J_{H-H} = 6.2 Hz), 6.43 (1.1H, d, $NC_5H_5(CH_2O)$, J_{H-H} = 7.9 Hz), 5.51 (2.1H, s(br), $NC_5H_5(CH_2O)$, J_{H-H} = 5.3 Hz), 1.38 (9.3H, s, $OC(CH_3)_3$). Elem anal. Calcd for $C_{20}H_{30}HfN_2O_4$ (MW = 540.95): C, 44.41; H, 5.59; N, 5.18. Found: C, 44.08; H, 5.46; N, 5.23.

[(μ-THME)(μ-OBu^t)Hf$_2$(OBu^t)$_4$]$_2$ ***(25)***. [Hf(OBu^t)$_4$] (0.40 g, 0.85 mmol) and H_3-THME (0.050 g, 0.42 mmol) in ~1.5 mL of tol. Yield: 82% (0.29 g). FTIR (KBr, cm^{-1}): 2968(s), 2922(m), 2865(m), 1458(m,br), 1406(m), 1383(m), 1358(m), 1206(s,br), 1128(m), 1066(m,sh), 1010(s,br), 917(w), 880(w), 781(w), 621(w), 485(s,br). Elem anal. Calcd for $C_{50}H_{108}Hf_4O_{16}$ (MW = 1679.36): C, 35.76; H, 6.48. Found: C, 36.16; H, 6.62.

General X-ray Crystal Structure Information.[24] Crystals were mounted onto a glass fiber from a pool of Fluorolube and immediately placed in a cold N_2 vapor stream, on a Bruker AXS diffractometer equipped with a SMART APEX CCD detector using graphite-monochromatized Mo Kα radiation (λ = 0.7107 Å). Lattice determination and data collection were carried out using *SMART*, version 5.054, software or the *APEXII* software suite. Data reduction and absorption correction were performed using either *SAINTPLUS*, version 6.01, software (absorption correction via the *SADABS* program within the *SAINT* software package) or the *APEXII* software suite (absorption correction performed using face indexing).

Structures were solved by direct methods that yielded the heavy atoms, along with a number of the lighter atoms, or by using the Patterson method, which yielded the heavy atoms. Subsequent Fourier syntheses yielded the remaining light-atom positions. The H atoms were fixed in positions of ideal geometry (riding model) and refined using *SHELXS* or *XSHELL*. The final refinement of each compound included anisotropic thermal parameters for all non-H atoms. All final

Table 2. Data Collection Parameters for 1−26

	1[c]	2	3	4	4a
chemical formula	$C_{20}H_{44}HfO_5$	$C_{26}H_{46}HfN_2O_4$	$C_{24}H_{48}HfN_4O_4$	$C_{64}H_{74}Hf_2O_{10}$	$C_{92}H_{104}Hf_4O_{16}$
fw	543.05	629.14	635.15	1360.21	2179.71
temp (K)	188(2)	173(2)	173(2)	193(2)	173(2)
space group	orthorhombic, *Cmc*2(1)	monoclinic, *Cc*	triclinic, $P\bar{1}$	monoclinic, *C*2/*c*	triclinic, $P\bar{1}$
a (Å)	11.2622(12)	12.4267(16)	9.4760(13)	17.841(2)	12.868(5)
b (Å)	19.504(2)	14.5716(18)	9.6926(14)	14.6484(16)	14.209(5)
c (Å)	12.2942(13)	16.503(2)	16.645(2)	24.992(3)	14.610(5)
α (deg)			94.277(2)		111.724(5)
β (deg)		96.077(2)	93.582(2)	96.5190(10)	103.867(5)
γ (deg)			100.798(2)		107.372(5)
V (Å^3)	2700.5(5)	2971.6(7)	1493.0(4)	6489.3(12)	2175.8(13)
Z	4	4	2	4	1
D_{calcd}(Mg/m^3)	1.256	1.406	1.413	1.392	1.664
μ,(Mo K*α*) (mm^{-1})	3.881	3.540	3.525	3.294	4.819
R1 (all data)[a] (%)	3.85 (5.10)	2.00 (2.06)	2.02 (2.06)	4.82 (8.17)	4.19 (5.97)
wR2 (all data)[b] (%)	9.99 (10.85)	5.05 (5.02)	4.96 (5.00)	12.17 (14.68)	10.11 (11.29)
	5	**5a**	**6**	**7**	**8**
chemical formula	$C_{42}H_{76}Hf_2O_8$	$C_{66}H_{94}Hf_3O_{11}$	$C_{82}H_{112}Hf_2O_{10}$	$C_{56}H_{72}Hf_2O_{10}$	$C_{52}H_{77}HfO_5$
fw	1066.01	1598.91	1614.70	1262.12	960.63
temp (K)	173(2)	188(2)	173(2)	193(2)	173(2)
space group	orthorhombic, *Pbca*	monoclinic, *P*21/*c*	triclinic, $P\bar{1}$	triclinic, $P\bar{1}$	monoclinic, *P*2(1)/*c*
a (Å)	20.414(3)	19.5770(13)	11.8206(6)	11.598(3)	13.0352(5)
b (Å)	19.223(3)	13.9040(9)	11.8510(6)	12.002(3)	13.5007(5)
c (Å)	24.999(4)	25.4289(17)	14.7547(8)	12.264(3)	27.8053(9)
α (deg)			81.465(2)	95.273(2)	
β (deg)		103.8040(10)	80.888(3)	111.814(3)	94.921(2)
γ (deg)			74.560(2)	102.161(3)	
V (Å^3)	9810(2)	6721.8(8)	1954.89(18)	1521.9(6)	4875.3(3)
Z	8	2	1	1	4
D_{calcd}(Mg/m^3)	1.444	1.574	1.372	1.377	1.309
μ,(Mo K*α*) (mm^{-1})	4.272	4.676	2.708	3.457	2.183
R1 (all data)[a] (%)	3.56 (5.75)	4.16 (7.67)	4.15 (5.65)	5.99 (7.04)	3.332 (6.19)
wR2 (all data)[b] (%)	11.31 (12.43)	7.77 (9.23)	10.41 (12.68)	15.10 (16.13)	9.21 (11.96)
	9	**10**	**11**	**13**	**14**[c]
chemical formula	$C_{30}H_{57}HfO_5$	$C_{36}H_{42}HfO_6$	$C_{34}H_{56}HfO_6$	$C_{36}H_{44}HfO_5$	$C_{44}H_{68}HfO_5$
fw	676.25	749.19	739.28	735.20	855.50
temp (K)	188(2)	188(2)	188(2)	188(2)	188(2)
space group	monoclinic, *P*2(1)/*m*	tetragonal, $P\bar{4}b2$	monoclinic, *P*2(1)/*n*	monoclinic, *P*2(1)/*c*	monoclinic, *P*2(1)/*n*
a (Å)	9.5174(5)	18.094(6)	14.8446(10)	12.0537(9)	10.926(7)
b (Å)	18.1890(10)	18.094(6)	15.2135(10)	35.859(3)	20.224(13)
c (Å)	10.3225(6)	10.231(3)	16.5388(11)	16.6506(13)	19.759(13)
β (deg)	102.9030(10)		104.2950(10)	103.8060(10)	91.281(7)
V (Å^3)	1741.83(17)	3349.3(19)	3619.4(4)	6989.0(9)	4365(5)
Z	2	4	4	8	4
D_{calcd}(Mg/m^3)	1.289	1.486	1.357	1.397	1.290
μ,(Mo K*α*) (mm^{-1})	3.025	3.157	2.920	3.022	2.429
R1 (all data)[a] (%)	2.22 (2.34)	5.21 (5.94)	2.83 (4.22)	3.41 (5.18)	13.17 (14.44)
wR2 (all data)[b] (%)	7.12 (7.51)	14.37 (15.52)	9.80 (11.82)	8.21 (9.08)	33.69 (34.17)
	15	**16**	**19**	**19a**	**20**
chemical formula	$C_{30}H_{56}HfO_5$	$C_{43}H_{42}HfN_3O_4$	$C_{42}H_{46}HfN_2O_4$	$C_{68}H_{74}Hf_2N_4O_8$	$C_{45}H_{65}HfNO_4$
fw	675.24	843.29	821.30	1432.29	862.47
temp (K)	188(2)	188(2)	173(2)	188(2)	188(2)
space group	monoclinic, *P*2(1)/*n*	orthorhombic, *Pbca*	orthorhombic, *Pbca*	monoclinic, *P*2(1)/*n*	monoclinic, *P*2(1)/*n*
a (Å)	12.0962(7)	18.942(3)	15.417(3)	11.8132(10)	12.6897(9)
b (Å)	17.8254(11)	14.616(2)	19.797(4)	18.9819(16)	18.8428(13)
c (Å)	15.7668(10)	27.444(4)	28.940(6)	16.0251(14)	18.9880(13)
β (deg)	93.7640(10)			103.3240(10)	105.1500(10)
V (Å^3)	3392.3(4)	7598(2)	8833(3)	3496.7(5)	4382.4(5)
Z	4	8	8	2	4
D_{calcd}(Mg/m^3)	1.322	1.474	1.235	1.360	1.307

dx.doi.org/10.1021/ic300622h | *Inorg. Chem.* 2012, 51, 12075−12092

Table 2. continued

	15	16	19	19a	20
μ,(Mo Kα) (mm^{-1})	3.106	2.791	2.398	3.018	2.419
R1 (all data)[a] (%)	3.20 (4.00)	7.78 (11.85)	4.85 (5.65)	2.49 (2.99)	3.41 (6.44)
wR2 (all data)[b] (%)	9.85 (10.94)	17.67 (20.30)	12.08 (12.46)	8.66 (9.39)	9.40 (12.37)
	21	**22**[c]	**23**	**24**	**25**
chemical formula	$C_{31}H_{53}HfNO_4$	$C_{34}H_{72}Hf_2O_{10}$	$C_{40}H_{60}Hf_2N_4O_8$	$C_{80}H_{120}Hf_4N_8O_{16}$	$C_{50}H_{108}Hf_4O_{16}$
fw	682.23	997.91	1081.90	2161.81	1679.32
temp (K)	188(2)	173(2)	173(2)	173(2)	173(2)
space group	monoclinic, $P2(1)/n$	monoclinic, $C2/c$	monoclinic, $P2(1)/c$	monoclinic, $P2(1)/c$	monoclinic, $C2/c$
a (Å)	19.892(5)	24.768(3)	20.6679(15)	15.339(2)	39.060(5)
b (Å)	17.489(5)	9.9099	9.6220(7)	18.253(2)	15.805(2)
c (Å)	19.892(5)	19.2242	24.0736(17)	16.805(2)	21.544(3)
β (deg)	98.82	113.452	111.5430(10)	102.467(2)	100.258(2)
V (Å^3)	6839(3)	4328.7(10)	4453.0(6)	4594.2(10)	13087(3)
Z	8	4	4	4	8
D_{calcd}(Mg/m^3)	1.325	1.346	1.614	1.508	1.705
μ,(Mo Kα) (mm^{-1})	3.081	4.830	4.710	4.562	6.380
R1 (all data)[a] (%)	5.06 (10.28)	12.88	3.89 (5.96)	3.16 (3.46)	2.30 (3.01)
wR2 (all data)[b] (%)	12.81 (15.65)	35.60	8.94 (10.08)	10.75 (11.12)	5.62 (6.29)

	26
chemical formula	$C_{60}H_{128}Hf_4O_{16}$
fw	1819.58
temp (K)	173(2)
space group	monoclinic, $C2/c$
a (Å)	18.564(2)
b (Å)	23.319(3)
c (Å)	18.727(2)
β (deg)	112.775(2)
V (Å^3)	7474.7(16)
Z	4
D_{calcd} (Mg/m^3)	1.617
μ,(Mo Kα) (mm^{-1})	5.592
R1 (all data)[a] (%)	2.37 (3.02)
wR2 (all data)[b] (%)	6.06 (6.72)

[a] $R1 = \sum||F_o| - |F_c||/\sum|F_o| \times 100$. [b] $wR2 = [\sum w(F_o^2 - F_c^2)^2/\sum(w|F_o|^2)^2]^{1/2} \times 100$. [c] Full structure not reported because of poor quality of the final structure model. Crystal unit cell data reported for convenience. If additional information is required concerning these structures, please contact the authors.

Table 3. Metrical Data for the OAr Derivatives

o-alkyl group	compd	nucl	Hf–OAr (av Å)	Hf–OBu^t (av Å)	Hf–HOBu^t (av Å)	Hf–solv (av Å)	OAr–Hf–OAr (av deg)	solv–Hf–OAr (av deg)	OBu^t–Hf–OAr (av deg)	OBu^t–Hf–OBu^t (av deg)
(CH_3)-2	**4**	2	2.02		2.290		98.24		115.54	
	10	1	1.98			2.26	94.76	87.05		
	16	1	1.98			2.39	109.35	113.96		
$CH(CH_3)_2$-2	**5**	2	2.20	1.91					111.38	102.57
	11	1	2.03	1.92		2.34	157.5	128.3	96.63	103.38
(CH_3)-2,6	**13**	1	1.94			2.29	97.19	105.75		
	19	1	1.98			2.40	117.71	106.5		
$CH(CH_3)_2$-2,6	**8**	1	1.95		2.32		112.3		128.4	
	14	1	1.96	1.91		2.26	109.53	106.5	110.1	
	20	1	1.955	1.90		2.42	106.5	106.2	112.2	
$C(CH_3)_3$-2,6	**9**	1	2.00	1.92	2.37				108.1	101.04
	15	1	1.99	1.92		2.38		104.8	112.2	100.2
	21	1	1.99	1.91		2.48		105.0	112.2	100.9

CIF files were checked at http://www.iucr.org/. Additional information concerning the data collection and final structural solutions can be found by accessing CIF files through the Cambridge Crystallographic Data Base. The data for the crystal structures of **1**–**26** have been deposited at the Cambridge Crystallographic Data Centre and allocated the deposition numbers CCDC 855821–855848. These data can be obtained free of charge from the Cambridge Crystallographic Data Centre, 12 Union Road, Cambridge CB2 1EZ, U.K. [fax (44) 01223-336033; e-mail deposit@ccdc.cam.ac.uk] or via http://www.ccdc.cam.ac.uk/conts/retrieving.html. Table 2 lists the data collection

Table 4. Metrical Data for the OAr/Oxide Derivatives

o-alkyl group	compd	nucl	Hf−OAr (av Å)	Hf−HOBu^t (av Å)	Hf−μ-O or Hf−μ-OH (av Å)	Hf---Hf (av Å)	OAr−Hf−OAr (av deg)	OR−Hf-OAr (av deg)	μ-O−Hf−μ-O (av deg)	solv−M− OAr (av deg)
(CH_3)-2	**4a**	4	1.97	2.21	(μ_3) 2.09, (μ) 2.15	3.358	99.42	92.67	72.33	
$CH(CH_3)_2$-2	**5a**	3	1.94		2.19	3.17	101.42	99.66	66.72	
$C(CH_3)_3$-2	**6**	2	1.97	2.27	2.13	3.54	96.82	115.6	69.46	
(CH_3)-2,6	**7**	2	1.97	2.26	2.15	3.52	99.41	115.5	69.45	
	19a	2	1.98		2.15	3.56	98.41		68.67	111.8

parameters for **1**−**26**. Tables 2−4 tabulate the metrical data (presented by ligand) for the OAr, OAr/oxide, and polydentate ligated compounds, respectively, isolated in this work.

Specific issues associated with individual structures are discussed below. The significant disorder observed for the pendant chains for **1**, **14**, and **22** resulted in resolution of the basic connectivity only. For compound **5a**, the disorder in the $OC_6H_4(CH(CH_3)_2)$-2 ligand led to it being refined isotropically, with no H atoms; however, the H atoms were added back into the molecular formula in the crystal (Table 2) to reflect charge neutrality. The molecular weights of compounds **4** and **6**−**10** reported in Table 2 reflect the final CIF files and do not include the protons detailed in the Experimental Section because they could not be unequivocally located in the final models. For **24**, three H atoms could not be located on one of the methyl groups of a disordered *tert*-butyl group but were added into Table 2 to maintain charge neutrality. The electron densities of disordered solvent molecules in the lattice were successfully modeled using the *PLATON*/*SQUEEZE* program for compounds **4**, **5**, **7**, **13**, **19**, and **19a**. The "squeezed" molecule atoms were not added to the molecular formula(s) in Table 2. Slightly disordered ligands were modeled using standard crystallographic restraints for **5**, **5a**, **15**, **24**, and **26**.

General Nanoparticle Synthesis. Under an argon atmosphere, a 0.5 M solution of the desired Hf precursor ([Hf(OBu^t)$_4$], **8**, **19a**, **22**, and **25**) in a mixture of oleic acid and oleylamine (2 mL/20 mL) was added to a Parr Acid Digestion bomb, sealed, transferred to an oven, and heated at 185 °C for 24 h. The nanomaterials were isolated by centrifugation followed by washing with acetone and toluene. The final nanoparticles could be dispersed with toluene.

Transmission Electron Microscopy (TEM). An aliquot of the HfO_2 nanopowder dispersed in toluene was placed directly onto a holey carbon type A, 200 mesh, copper TEM grid that was purchased from Ted Pella, Inc. The aliquot was then allowed to dry. The resultant particles were analyzed using a Philips CM 30 transmission electron microscope operating at 300 kV accelerating voltage and equipped with a Thermo Noran System 6 energy-dispersive X-ray system operating at 300 kV accelerating voltage.

Powder X-ray Diffraction (PXRD). Powder samples were mounted directly onto a zero background holder (The Gem Dugout). The average Bravais lattice crystal symmetry and cell parameters were found using PXRD patterns collected on a PANalytical powder diffractometer with Cu Kα radiation (1.5406 Å) and an RTMS X'Celerator detector. Patterns were analyzed with the *JADE* software program.[25]

RESULTS AND DISCUSSION

A search of the crystallographically characterized compounds that possess one Hf and four OR ligands yields a surprisingly small set of compounds.[12] Removing compounds from this list that possess problematic anions for oxide materials production[26,2728−32] or oxo-containing species[33,34] leaves only a handful of "simple" [Hf(OR)$_4$] that have been fully characterized, including [Hf(OPr^i)$_4$·HOPr^i],[13] [Hf(OPr^i)$_4$(solv)]$_2$ [solv = HOPr^i or HOPr^i/py],[14] and [(MMPO^e)$_2$Hf(OR)$_2$] (OR = OBu^t,[15] MMPO[16] or methoxy-2-methyl-2-propanolato). Recently, we added to this family of compounds using the ONep ligand: {[H][(μ-ONep)$_3$Hf$_2$(ONep)$_5$(OBu^t)]}.[35] From this limited number of simple [Hf(OR)$_4$] precursors, only monomeric or dinuclear species have been reported. Because of this void, a great deal of [Hf(OR)$_4$] precursor development was warranted prior to our investigation into HfO_2 nanomaterials.

The following discussion is organized by characterization of the following: (A) solvates, unraveling the structural impact on [Hf(OBu^t)$_4$] from a series of Lewis basic solvents (i.e., THF, py, and MeIm); (B) phenoxides, attempts to determine the extent of aryloxide substitution and structural impact, further subdivided by solvent (i) toluene, (ii) THF, and (iii) py; (C) complex polydentate, alkoxide ligands to induce additional structural variants; (D) nanoparticle synthesis, first route to employ [Hf(OR)$_4$] precursors and a preliminary investigation into the applicability of the PSA[4,9,10] on generating morphologically controlled HfO_2 nanoparticles.

A. Solvates (1−3). The solution molecular complexity of [Hf(OBu^t)$_4$] has not been reported but was considered to be monomeric in toluene based on the fact that [Ti(OBu^t)$_4$] and [Zr(OBu^t)$_4$] reportedly have a molecular complexity of 1.0,[11] the similarity in size of Zr^{4+} and Hf^{4+},[36] and that hafnium tertiary alkoxides possess greater volatility than zirconium or titanium.[11] Therefore, it was assumed that [Hf(OBu^t)$_4$] in Lewis basic solvents would yield monomeric complexes. The addition of a Lewis base to [Hf(OBu^t)$_4$] immediately formed a white precipitate, which facilely dissolved with heating. Upon cooling, crystals of the monomeric solvates of THF (**1**), py (**2**), and MeIm (**3**), shown in Figure 2a−c, respectively, were formed. Compounds **1** and **3** represent the first THF and MeIm solvate derivatives of [Hf(OR)$_4$]. Previously, the only monomeric [Hf(OR)$_4$] complex reported employed the polydentate MMPO ligand.[15,16] While the quality of the crystal structure solution for **1** (ball and stick shown in Figure 2a) was poor, the connectivity unequivocally established it as a five-coordinated monomer. Upon drying under vacuum, crystals of **1** re-formed a clear liquid, which was attributed to the loss of the weakly bound THF solvent molecule. This volatility explains the difficulty in obtaining high-quality single crystals, the lower than expected yield after drying the crystals, and poor elemental analysis results. The only other structurally characterized five-coordinated hafnium compounds reported that are bound solely by O atoms are the siloxides: [Hf((μ-OBu^t)OSi(OBu^t)$_2$)]-[Hf(OSi(OBu^t)$_3$)$_4$][37] and [Hf(OSi(OBu^t)$_3$)$_4$(H$_2$O)].[38]

In contrast to **1**, compounds **2** and **3** were solved as six-coordinated, pseudooctahedrally (OC-6) coordinated monomers. This was achieved by the binding of two solvent molecules. While the previously reported [Hf(OPr^i)$_4$(py)]$_2$[14] derivative was isolated as a dimer, the nuclearity variation is attributed to the decreased steric bulk of OPr^i versus OBu^t. The yield of **3** was initially higher than calculated because of the difficulty in removing excess MeIm from in vacuo drying. After numerous washings with hexanes and toluene, the product weight was constant but led to a reduction in the overall yield, presumably because of lost product. Elemental analyses of **2** and **3** were found to be incongruous with the calculated values, which was

dx.doi.org/10.1021/ic300622h | *Inorg. Chem.* 2012, 51, 12075−12092

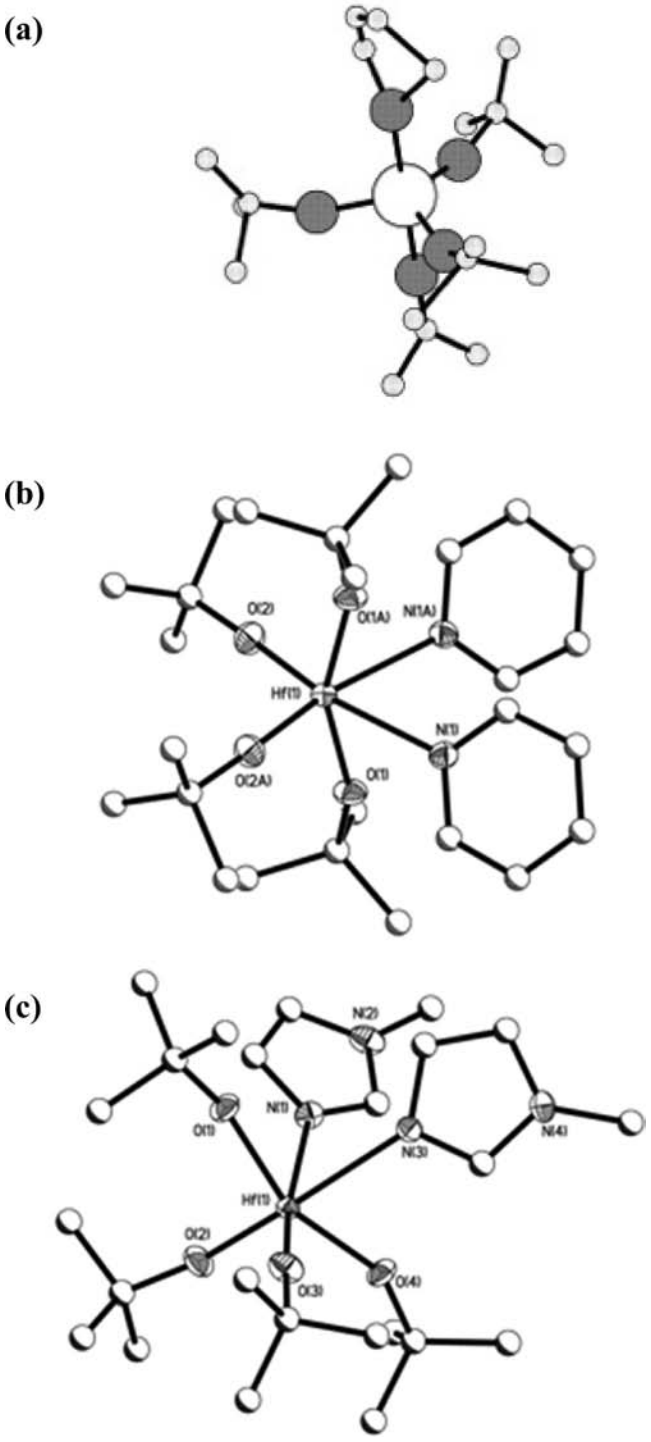

Figure 2. Structure plots of solvates: (a) **1** (ball and stick); (b) **2**; (c) **3**. Thermal ellipsoids of heavy atoms drawn at the 30% level with C atoms drawn as ball and stick for clarity.

attributed to the volatility of the bound solvent at the high temperatures used for analysis. The metrical data indicate that **2** and **3** possess similar Hf–O bond distances (1.96 and 1.98 Å, respectively) and are in agreement with those reported for the $[(MMPO^e)_2Hf(OBu^t)_2]$[15] (av 1.93 Å) complex. The Hf–N_{solv} distances of 2.45 and 2.40 Å for **2** and **3**, respectively, are also consistent with those noted for other Hf–N distances (range 2.06[39]–2.46[40] Å).[12] The FTIR spectrum of **1**–**3** displayed a strong peak around 990 cm^{-1}, which is consistent with the ν(C–O)Hf.[41] The ν(Hf–O) stretch is reported to be at 567 and 526 cm^{-1} and was observed in both **1** and **2** but not **3**. This is attributed to the influence of the strong Lewis base MeIm solvate, where the introduction of coordinating solvents has been reported to shift M–O bands to lower frequencies.[41] NMR data for **1** and **2** revealed the single OBu^t resonance in the parent deuterated solvent; however, compound **3** was surprisingly not soluble enough in py-d_5 or $CDCl_3$ to garner an acceptable NMR spectrum.

From this simple set of compounds, the monomeric nature of $[Hf(OBu^t)_4]$ in the presence of a Lewis basic solvent has been verified. Therefore, modification of this precursor with the more sterically demanding OAr ligands was expected to yield monomeric species as well in Lewis basic solvents; however, nonpolar solvents were not as predictable.

B. Phenoxide Derivatives. The synthesis of this series of OAr-modified $[Hf(OBu^t)_4]$ compounds was undertaken using commercially available, sterically varied, 2,6-substituted phenols (HOAr, eq 1). The Hf-OAr derivatives were of interest because the steric bulk around the metal center can be easily manipulated based on the ortho substitution. The series of solvents investigated included (i) toluene, (ii) THF, and (iii) pyridine, and the products are discussed in order below. Figures 3–8 show the thermal structure plots of the various ligand/solvent systems for $HOC_6H_4(R)$-2 where R = CH_3 (Figure 1b), $CH(CH_3)_2$ (Figure 1c), and $C(CH_3)_3$ (Figure 1d) and for $HOC_6H_3(R)_2$-2,6 where R = CH_3 (Figure 1e), $CH(CH_3)_2$ (Figure 1f), and $C(CH_3)_3$ (Figure 1g), respectively.

*i. Toluene Products (**4**–**9**).* Initial efforts focused on generating the fully substituted compounds using toluene as the solvent (eq 1). After stirring for 12 h, the resulting modified $[Hf(OR)_4]$ products were isolated by crystallization. For the majority of samples, the loss of the broad –OH stretch around 3000 cm^{-1} and/or the inclusion of OAr stretches and bends in the FTIR spectra of these crystals indicated that some degree of substitution had occurred. A strong peak around 1000 cm^{-1} was noted in each spectrum, which is consistent with ν(C–O)Hf,[41] but the ν(Hf–O) stretches noted for Nujol samples of $[Hf(OBu^t)_4]$[41] were not readily observed for all samples. For **7** and **8**, in addition to the OAr stretches and bends, a broad stretch around 3500 cm^{-1} was observed, indicating the presence of a hydroxide or phenol moiety; however, there was no stretch noted in this range for **4**, **6**, or **9**, which were solved (vide infra) as a $HOBu^t$ derivative.

To assist in understanding the various structural changes wrought from these substitutions, single-crystal X-ray studies were undertaken and are discussed below based on increasing steric bulk of the OAr ligand. For a number of the compounds synthesized in this study, more ligands are present than can be accounted for by the tetravalent nature of the Hf metal center. This requires the assignment of H atoms in the final structure, but unambiguous assignment of their proper location was not always possible. While the delocalized protons can be placed outside of the formula as we did for $[H][(\mu\text{-}ONep)_3Hf_2(ONep)_5(OBu^t)]$,[35] we have attempted to identify their location based on metrical data, literature structures, and logical deduction. The source of the oxide/hydroxide moiety identified in the following structures is currently unknown; however, oxo species are prevalent in the synthesis of $[M(OR)_x]$ and reportedly produced by several mechanisms including hydrolysis due to adventitious water, ligand degradation (i.e., ether, ester, or alkene elimination), and aerobic oxidation.[11,41] Each of these routes has been considered for the toluene system, but a great

dx.doi.org/10.1021/ic300622h | *Inorg. Chem.* 2012, 51, 12075–12092

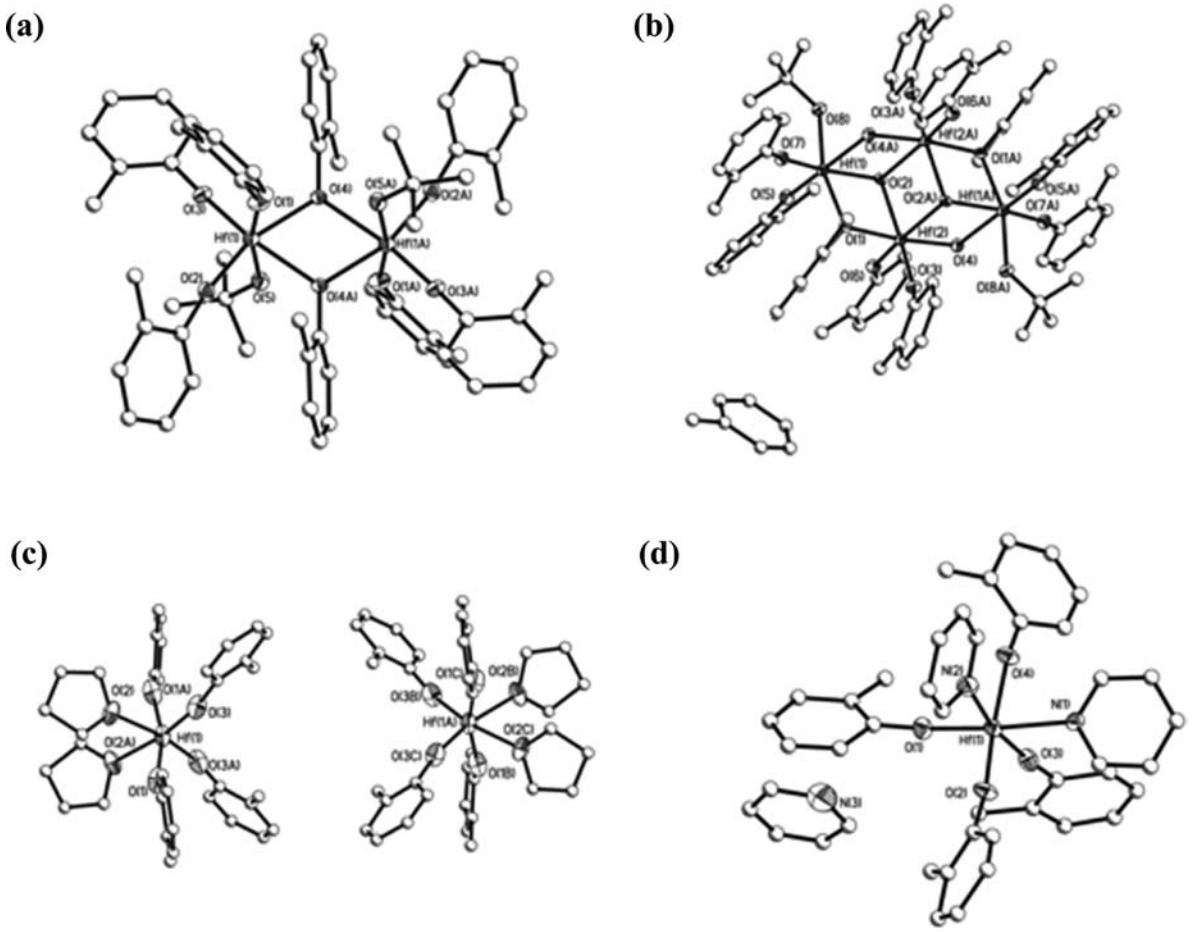

Figure 3. Structure plots of $OC_6H_4(CH_3)$-2 phenoxide derivatives: (a) **4**; (b) **4a**·tol; (c) **10** (two molecules per unit cell); (d) **16**. Thermal ellipsoids of heavy atoms drawn at the 30% level with C atoms drawn as ball and stick for clarity.

deal more work is necessary to verify the proper mechanism(s) for formation of the oxo moiety. The structures isolated from toluene are discussed below according to (a) the 2-monosubstituted and the (b) 2,6-disubstituted OAr derivatives.

a. Monosubstituted OAr Derivatives (4–6). The mono-ortho-substituted OAr derivatives of $[Hf(OBu^t)_4]$ (Figure 1b–d) were all found to form dinuclear complexes. Compound **4** had two pseudo-OC-6-bound Hf metal centers that were bridged by two μ-$OC_6H_4(CH_3)$-2 ligands (see Figure 3a). The remaining coordination sites were filled by six terminal $OC_6H_4(CH_3)$-2 and two OBu^t ligands. Charge balance requires that two of these ligands are protonated. Because the axial Hf–OBu^t distances of 2.29 Å for **4** (see Table 3) were significantly longer than those observed for **2** and **3** (av 1.97 Å), they were assigned as $HOBu^t$ ligands. The structure of **4** is similar to constructs of $[M(OPr^i)_4(HOPr^i)]_2$ (M = Zr,[42,43] Hf[14]), which also possess distinguishing, longer, axial M–$HOPr^i$ distances (i.e., Hf–$HOPr^i$ = av 2.21 Å[14]). During one attempt to recrystallize **4** from a protracted crystal growth, the oxo species **4a**·tol (Figure 3b) was generated. This compound adopts a M_4O_{16} structure, with two μ_3-O, two μ-O, and two μ-$OC_6H_4(CH_3)$-2 holding the central core together. In addition, there are four $OC_6H_4(CH_3)$-2 and two OBu^t terminal ligands. To maintain charge neutrality, based on the metrical data (Table 4) and what is typically reported for solvated M_4O_{16} structures,[12] the OBu^t ligands were formally protonated and the bridging oxide ligands were assigned as a μ-OH.

Using the more sterically demanding $OC_6H_4(CH(CH_3)_2)$-2 ligand led to the dinuclear complex **5** (see Figure 4a), which had successfully metathesized only one OBu^t ligand. The resulting Hf metal centers adopted a distorted square-base-pyramidal (SBP; τ = 0.21) geometry, using two μ-$OC_6H_4(CH(CH_3)_2)$-2 ligands and three terminal OBu^t ligands per metal. The metrical data (Table 3) are consistent with the other compounds in this investigation. One attempt to generate higher-quality crystals from a slower growth process led to the formation of the oxo species **5a**. The structure of **5a** adopts a standard M_3O_{12} arrangement with two μ_3-O, three μ-OBu^t, and six terminal $OC_6H_4(CH(CH_3)_2)$-2 ligands (shown in Figure 4b). The necessary phenol(s) or hydroxide(s) ligands could not be discerned from the metrical data (Table 4) or from $Hf_3(\mu_3$-O) literature compounds[12,33,44,45] and were therefore considered distributed around the molecule.

All attempts to generate a Hf-$OC_6H_4(C(CH_3)_3)$-2 derivative led to isolation of the oxo species **6** (Figure 5), with two toluene molecules located in the unit cell. This compound adopts a standard M_2O_{10} dinuclear arrangement with two μ-O, six terminal $OC_6H_4(C(CH_3)_3)$-2, and two terminal OBu^t ligands. In agreement with the similar literature structures[46–49] and confirmed by the metrical data (Table 4), the complex was assigned as μ-OH with an axial $HOBu^t$ ligand. Interestingly, the FTIR data do not reveal the expected strong –OH stretch around 3500 cm^{-1}, but this may be a reflection of the bridging nature of μ-OH.

dx.doi.org/10.1021/ic300622h | *Inorg. Chem.* 2012, 51, 12075–12092

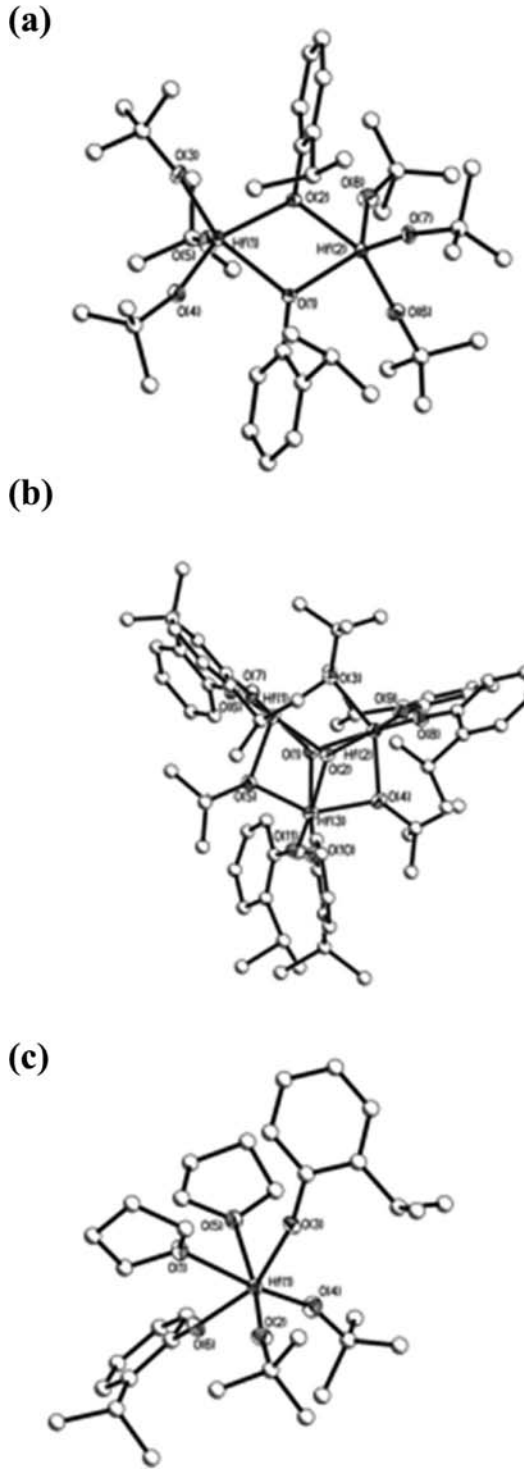

Figure 4. Structure plots of $OC_6H_4(CH(CH_3)_2)$-2 phenoxide derivatives: (a) **5**; (b) **5a**; (c) **11**. Thermal ellipsoids of heavy atoms drawn at the 30% level with C atoms drawn as ball and stick for clarity.

Elemental analyses were undertaken to further determine the purity of the bulk powders of **4**–**6**. It is of note that for $[M(OR)_x]$ it is often difficult to obtain acceptable analyses because of the properties that make them of interest for materials applications: low decomposition temperatures, high volatility, rapid hydrolysis, and inclusion of solvents (i.e., increased solubility). Therefore, it is not surprising that most of the experimental data are not consistent with the calculated percentages. For both **4** and **5**,

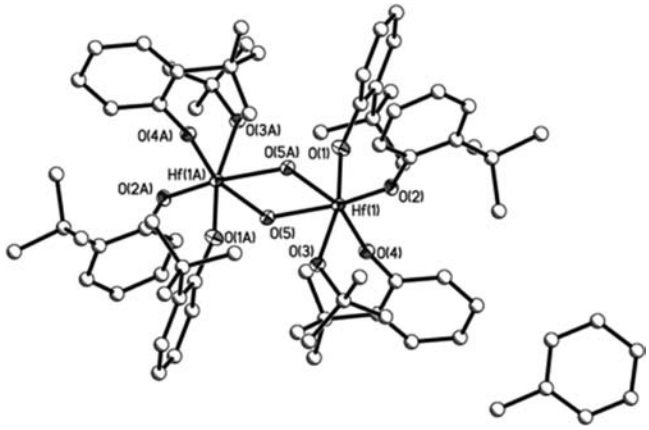

Figure 5. Structure plot of $OC_6H_4(C(CH_3)_3)$-2 phenoxide derivative **6**. Thermal ellipsoids of heavy atoms drawn at the 30% level with C atoms drawn as ball and stick for clarity.

the obtained percentages are in agreement with the loss of ligand moieties similar to what was observed for the oxide crystal structures of **4a** and **5a**, respectively. The simple ^{1}H NMR spectra obtained for **4** and **5** in $CDCl_3$ were consistent with the observed crystal structure; however, the low solubility of these compounds prevented the collection of useful ^{13}C NMR spectra. For **6**, the removal of a toluene solvent molecule from the formula leads to acceptable percentages.

*b. Disubstituted Derivatives (**7**–**9**).* Modifying $[Hf(OBu^t)_4]$ with the 2,6-disubstituted OAr ligands (Figure 1e–g) was initiated using $HOC_6H_3(CH_3)_2$-2,6; however, only oils were isolated. From a long-time reaction mixture, **7** (Figure 6a) was solved as a dinuclear species with a metal center that uses three terminal $OC_6H_3(CH_3)_2$-2,6, two bridging O atoms, and one terminal OBu^t ligand. The metrical data (Table 4) for **7** are consistent with a $[Hf(\mu\text{-}OH)]_2$ central core and a $HOBu^t$ ligand.[44,46–54] For the $OC_6H_3(CH(CH_3)_2)_2$-2,6 (**8**; Figure 7a) and $OC_6H_3(C(CH_3)_3)_2$-2,6 (**9**; Figure 8a) derivatives, oxo-free monomers were identified. Compound **8** was solved in an irregular SBP (τ = 0.12)[55] arrangement using four $OC_6H_3(CH(CH_3)_2)_2$-2,6 and one OBu^t ligand. Compound **9** possesses only a single $OC_6H_3(C(CH_3)_3)_2$-2,6 with retention of four OBu^t ligands, forming a very distorted SBP (τ = 0.41) geometry around the Hf metal center. For both **8** and **9**, the substantially longer Hf–OBu^t distance observed in **8** [Hf(1)–O(8) = 2.32 Å] and **9** [Hf(1)–O(3) = 2.37 Å] allows for these ligands to be assigned as a charge-balancing alcohol ($HOBu^t$). Elemental analyses of the crystalline material of **7** (when two toluene molecules are included) and **9** were found to be in agreement with the calculated values. For **8**, the conversion of several ligands [$HOBu^t$ and one $OC_6H_3(CH(CH_3)_2)_2$-2,6 ligand] to –OH results in acceptable values.

Further characterization of the bulk powders of **7**–**9** using ^{1}H and ^{13}C NMR spectroscopy was undertaken in tol-d_8. Again, the compounds' low solubility prevented useful information from being obtained for the ^{13}C NMR spectra; however, the ^{1}H NMR data did lend some insight into their purity. For the ^{1}H NMR spectrum of **7**, three sets of resonances were expected for the –OH, $OC_6H_3(CH_3)_2$-2,6, and $HOBu^t$ ligands. The latter two resonances were observed but were overlapped with the tol-d_8 peaks, which makes accurate integration difficult. The OH resonance was not unequivocally observed. For **8**, the methyl resonances of $OC_6H_3(CH(CH_3)_2)_2$-2,6 to the OBu^t resonances were found to be in rough agreement with a 15.5:3 ratio

dx.doi.org/10.1021/ic300622h | *Inorg. Chem.* 2012, 51, 12075–12092

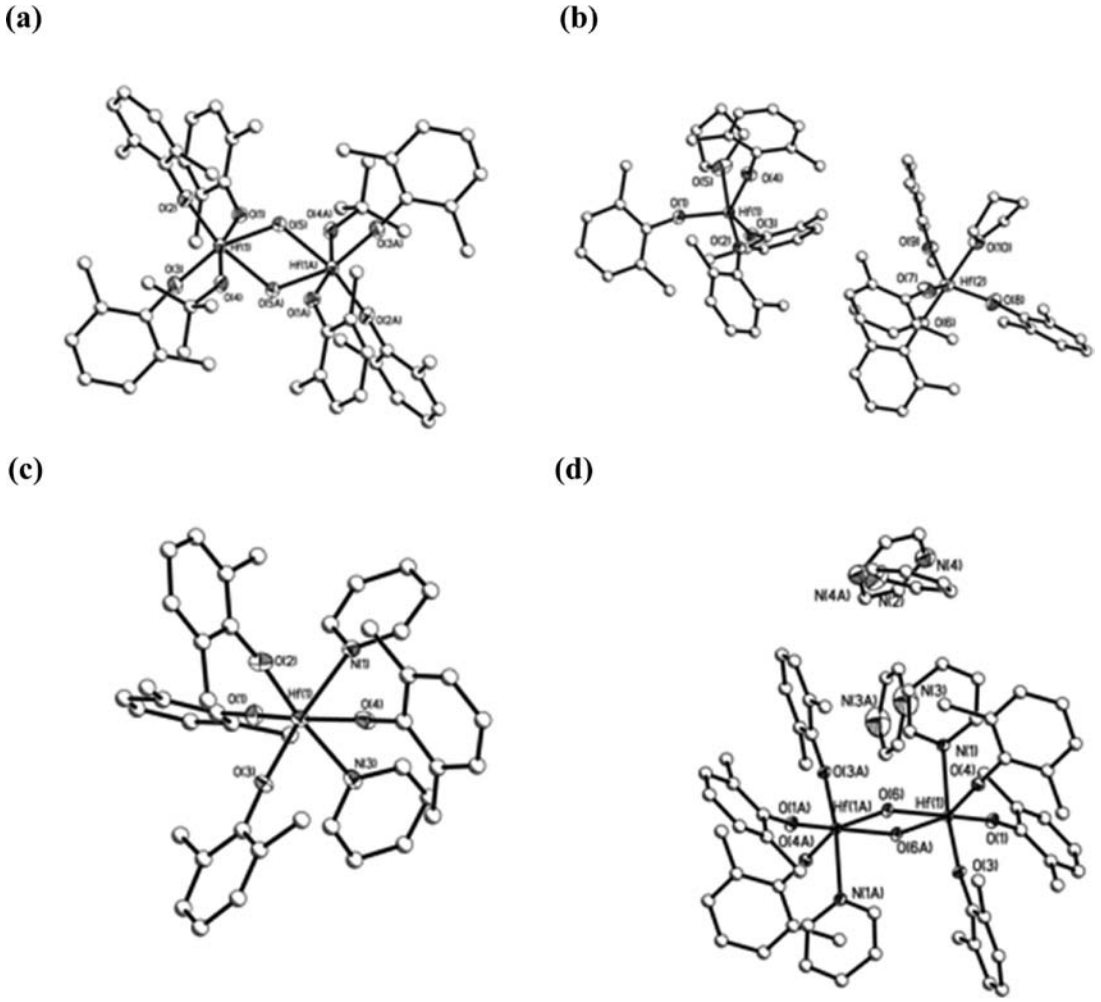

Figure 6. Structure plots of $OC_6H_3(CH_3)_2$-2,6 phenoxide derivatives: (a) **7**; (b) **13** (two molecules per unit cell); (c) **19**; (d) **19a**. Thermal ellipsoids of heavy atoms drawn at the 30% level with C atoms drawn as ball and stick for clarity.

compared to the expected 16:3 ratio. For **9**, the spectrum in $CDCl_3$ showed the expected 1:4 $OC_6H_3(C(CH_3)_3)$-2,6 to OBu^t ratio. The NMR data coupled with the acceptable elemental analyses argue for an agreement between the observed structure of **7**−**9** and the bulk powder.

*ii. Tetrahydrofuran Derivatives (**10**−**15**).* The introduction of THF was expected to reduce the nuclearity of the compounds based on the expected coordination of the Lewis basic solvent. In contrast to the toluene derivatives, the FTIR data for the THF adducts (**10**−**15**) had no −OH stretches and the remaining stretches and bends were noticeably less complicated but fully consistent with the various OAr ligands investigated. The ν(C−O)Hf and ν(Hϕ−O) stretching frequencies of the THF versus toluene derivatives were slightly shifted. The degree of substitution could not be unequivocally established, and crystal structures were obtained when possible to understand the modifications.

The $OC_6H_4(CH_3)$-2 ligated compound **10** (Figure 3c) was solved as a fully substituted mononuclear species, generating an OC-6 Hf metal center by also binding two THF solvent molecules. Two molecules were solved in the unit cell. As the steric bulk was slightly increased, only the disubstituted species **11** was formed (see Figure 4c). Again, the hafnium adopts a pseudo-OC-6 arrangement using two $OC_6H_4(CH(CH_3)_2)$-2, two OBu^t, and two THF molecules. All attempts to generate the $OC_6H_4(C(CH_3)_3)$-2-ligated species yielded only oils. The $OC_6H_3(CH_3)_2$-2,6 derivative **13** (Figure 6b) was found to be a fully substituted monomer that also binds a single THF solvent molecule, thereby generating a distorted, trigonal-bipyramidal (TBP; τ = 0.59) coordination around the hafnium. Employing the larger $OC_6H_3(CH(CH_3)_2)_2$-2,6 ligand led to **14** (Table 2), which because of poor crystal quality could only have its connectivity identified as $[Hf(OC_6H_3(CH(CH_3)_2)_2\text{-}2,6)_3(OBu^t)(THF)]$. Finally, the steric bulk of the $OC_6H_3(C(CH_3)_3)_2$-2,6 modifier allowed for only one successful ligand substitution, forming **15** (Figure 8b). In addition, one THF solvent molecule bound to the Hf metal center, yielding a pseudo-SBP (τ = 0.37) geometry.

The solution state of the THF adducts was investigated through ^{1}H NMR studies using crystals of **10**−**15** individually dissolved in THF-d_8. For the majority of compounds, the appropriate signals for the ligands (OAr/OBu^t) in the ratio noted in the solid state were observed in the ^{1}H NMR spectrum. For **11**, the OBu^t peaks were not readily discernible, but on the basis of integration of the doublet for the propyl group of the $OC_6H_4(CH(CH_3)_2)$-2 ligand, it is apparent that these peaks coincidentally overlap. Peaks consistent with the free $HOC_6H_4(CH(CH_3)_2)$-2 ligand were present in the spectrum at low levels, which is consistent with the elemental analysis data (vide infra). We were not able to successfully grow crystals of

dx.doi.org/10.1021/ic300622h | *Inorg. Chem.* 2012, 51, 12075−12092

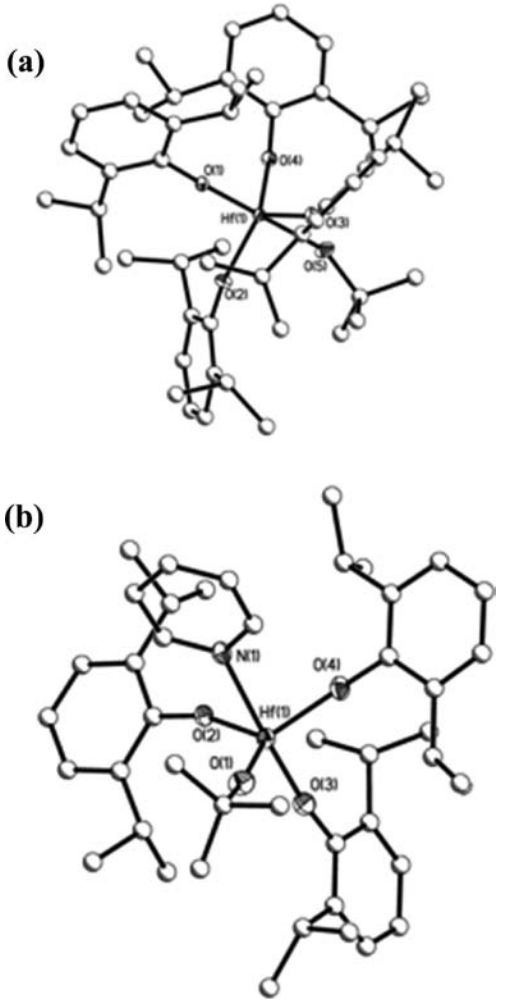

Figure 7. Structure plots of $OC_6H_3(CH(CH_3)_2)_2$-2,6 phenoxide derivatives: (a) **8**; (b) **20**. Thermal ellipsoids of heavy atoms drawn at the 30% level with C atoms drawn as ball and stick for clarity.

the $OC_6H_4(C(CH_3)_3)$-2 derivative **12**. Experimental elemental analyses obtained for **10** and **13** were found to be in agreement with the calculated values. For **11**, it appears that the variation may be due to the inclusion of residual $HOC_6H_4(CH_3)$-2 solvent molecules. For **15**, the variation is more in line with the premature loss of the $OC_6H_3(C(CH_3)_3)_2$-2,6 ligand.

iii. Pyridine Derivatives (16–21). When py was used as the solvent (eq 1), the FTIR spectra of the various products (**16**–**21**) appeared to be very similar to the previously discussed THF adducts. Again, the −OH peaks were not observed in these spectra and the ν(C−O)Hf and ν(Hϕ−O) stretching frequencies were slightly shifted in comparison to the tol or THF system. Crystal structures were obtained for each reaction mixture when possible, and all nonoxide species were isolated as solvated monomers.

For the $OC_6H_4(CH_3)$-2 derivative, monomeric **16** (see Figure 3d) had an OC-6 Hf metal center [four $OC_6H_4(CH_3)$-2 ligands and two py solvent molecules] similar to what was noted for the THF adduct **10**. An additional molecule of py was located within the unit cell for **16**. Both the $OC_6H_4(CH(CH_3)_2)$-2 (**17**) and $OC_6H_4(C(CH_3)_3)$-2 (**18**) derivatives formed oils, and thus crystal structures were not available. For the disubstituted species, the $OC_6H_3(CH_3)_2$-2,6 derivative yielded compound **19** (Figure 6c), which displayed full ligand substitution.

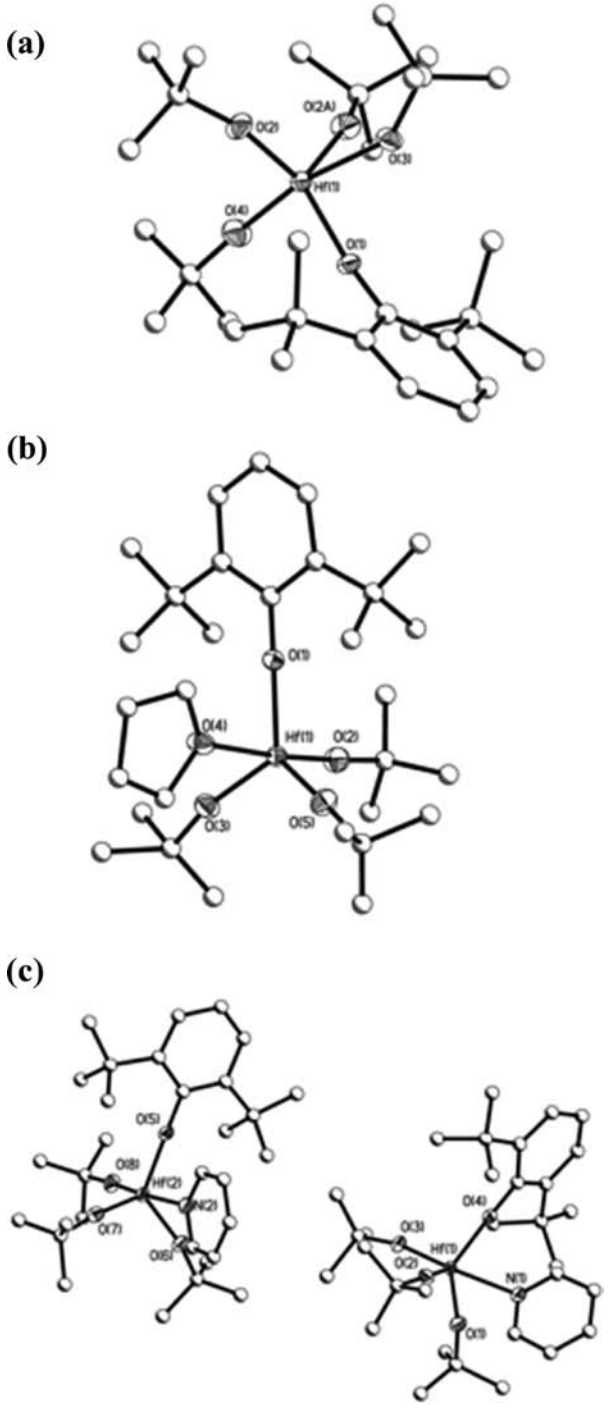

Figure 8. Structure plots of $OC_6H_3(C(CH_3)_3)$-2,6 phenoxide derivatives: (a) **9**; (b) **15**; (c) **21** (two molecules per unit cell). Thermal ellipsoids of heavy atoms drawn at the 30% level with C atoms drawn as ball and stick for clarity.

The pseudo-OC-6 geometry was generated through the binding of two py solvent molecules, as shown in Figure 6c. A long-term crystallization mixture led to the dinuclear species **19a** (Figure 6d), where each hafnium possesses three $OC_6H_3(CH_3)_2$-2,6 ligands, a py (Hf−N_{py} = 2.42 Å), and a bridging OH ligand. Again, the assignment of an −OH in the structure is consistent with the metrical data (Table 4) and literature reports.[23,26,44,46,48−54,56−58] Increasing the steric bulk to the $OC_6H_3(CH(CH_3)_2)_2$-2,6 ligand allows for three ligand substitutions,

dx.doi.org/10.1021/ic300622h | *Inorg. Chem.* 2012, 51, 12075−12092

Table 5. Substitution Number of the OAr Ligands[a]

	$OC_6H_4(R)$-2			$OC_6H_3(R)$-2,6		
solvent/R	CH_3	$CH(CH_3)_2$	$C(CH_3)_3$	CH_3	$CH(CH_3)_2$	$C(CH_3)_3$
tol	4 (**4**)	1 (**5**)	3 (**6**, oxo)	3 (**7**, oxo)	4 (**8**)	1 (**9**)
THF	4 (**10**)	2 (**11**)	–	4 (**13**)	3 (**14**)	1 (**15**)
py	4 (**16**)	–	–	3 (**19**)	3 (**20**)	1 (**21**)
				3 (**19a**, oxo)		

[a]Compound number listed in parentheses. – = compound not isolated.

yielding a distorted SBP geometry (τ = 0.31) for **20** (Figure 7b) through coordination of a py solvent molecule. The OC_6H_3-$(C(CH_3)_3)_2$-2,6 reaction (eq 1) again formed the monosubstituted complex, forming an irregular SBP (τ = 0.33) geometry for the hafnium of **21** (Figure 8c; two molecules per unit cell).

Elemental analyses for the py adducts **16** and **19**–**21** were not in agreement with the proposed values. For all of these compounds, the addition or subtraction of py solvent molecules will place the obtained values in the acceptable range. Again, crystalline material was dissolved in the parent deuterated solvent (i.e., py-d_5 for **16**–**21**) to elucidate structural behavior and purity. For the monomeric py adduct (**16** and **19**–**21**), not surprisingly only one set of ligands was noted for these compounds, which argues for retention of their structure in solution.

iv. Metrical Data. Metrical data of the OAr (tol, THF, and py) derivatives are listed in Table 3 by ligand. As can be discerned, the bond distances and angles of this family of compounds are self-consistent. The two dinuclear OAr derivatives (**4** and **5**) possessed Hf---Hf distances of 3.38 and 3.57 Å and μ-OAr–M–μ-OAρ angles of 70.72° and 66.52°, respectively. The average Hf–OAr distance is 2.00 Å, which is longer than the average Hf–OBu^t distance of 1.92 Å. In contrast, the ligands that were assigned as HOBu^t have Hf–O distances that average 2.33 Å, which is in line with other solvates (THF and py) with a Hf–solv distance of 2.37 Å. Coordination around the hafnium metal was individually discussed above, and it was found that the majority of five-coordinated species were distorted SBP, with the six-coordinated complexes adopting pseudo-OC-6 geometries.

v. Structural Ligand Effect Summary. It was originally thought that the substitution pattern of OAr for OBu^t would be directed by the steric bulk of the ortho substituent(s) and the pK_a[59] of the phenol [i.e., (CH_3)-2 < $(CH(CH_3)_2)$-2 < $(C(CH_3)_3)$-2 < $(CH_3)_2$-2,6 < $(CH(CH_3)_2)_2$-2,6 < $(C(CH_3)_3)_2$-2,6]. Table 5 shows the general metathesis that occurred in the solvents employed (eq 1). At the extremes, the steric bulk trend holds, where, independent of the solvent used, the OC_6H_4-(CH_3)-2 derivatives (Figure 3) demonstrate full exchange while the $OC_6H_3(C(CH_3)_3)_2$-2,6 system (Figure 8) generates only one substitution. The rest of the ligands do not appear to follow any specific trend. The $OC_6H_4(CH(CH_3)_2)$-2 derivatives demonstrated limited metathesis, while the more sterically demanding $OC_6H_4(C(CH_3)_3)$-2 (Figure 5), $OC_6H_3(CH_3)_2$-2,6 (Figure 6), and $OC_6H_3(CH(CH_3)_2)_2$-2,6 (Figure 7) products had three or four exchanged products. This alters the exchange pattern to (CH_3)-2 > $(C(CH_3)_3)$-2 ~ $(CH_3)_2$-2,6 ~ $(CH(CH_3)_2)_2$-2,6 > $(CH(CH_3)_2)$-2 > $(C(CH_3)_3)_2$-2,6. It is also of note that each molecule had sufficient room to bind at least one solvent ligand for the THF or py systems. Therefore, it is clear that the substitution behavior is more complex than being dependent on either the steric bulk of the ortho substituent or the acidity of the phenol protons. However, these compounds set the framework for a more in-depth study that is necessary to understand and control substitution of these HOAr with $[Hf(OBu^t)_4]$.

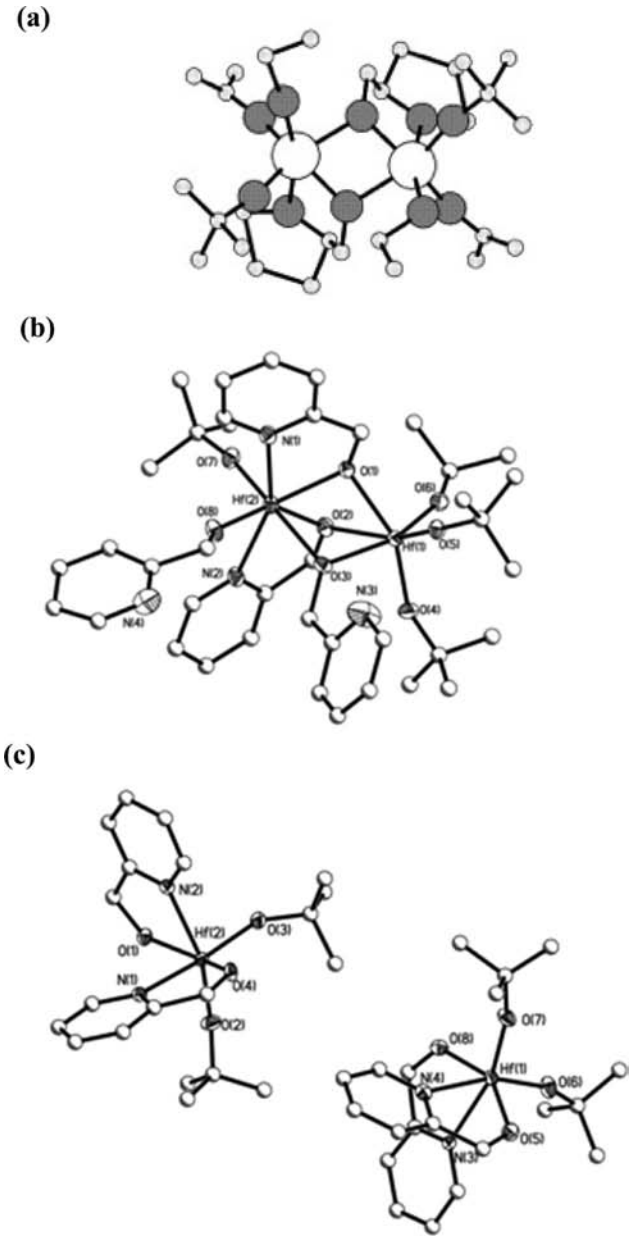

Figure 9. Structure plots of OR* derivatives: (a) **22** (ball and stick); (b) **23**; (c) **24** (two molecules per unit cell). Thermal ellipsoids of heavy atoms drawn at the 30% level with C atoms drawn as ball and stick for clarity.

C. Complex Polydentate Alcohols (22–26). Because compounds **1**–**21** were monomeric or dimeric, it was of interest to explore whether the polydentate alcohols could generate

dx.doi.org/10.1021/ic300622h | *Inorg. Chem.* 2012, 51, 12075–12092

Table 6. Metrical Data for the Polydentate Derivatives

ligand	compd	nucl	M−OL (av Å)	M−OBu^t (av Å)	M---M (av Å)	OL−M−OL (av deg)	OBu^t−M−OBu^t (av deg)	OBu^t−M−OL (av deg)	μ-OL−M−OBu^t (av deg)	μ-OL−M−μ-OL (av deg)
OPy	**23**	2	(O) 2.00 (μ-O) 2.17 (N) 2.40	1.93	3.27	(N) 155.2	102.23	100.4	116.6	71.45
	24	1	(O) 2.04 (N) 2.38	1.94	–	(N) 78.73 (O) 148.7	103.1	(N) 126.0 (O) 99.5	–	
THME	**26**	4	2.15	(O) 1.96 (μ-O) 2.20	3.52	77.89	96.58	–	(O) 124.8 (μ-OBu^t) 69.96	85.12
	27	4	2.14	(O) 1.94 (μ-O) 2.19	3.49	90.58	94.25	–	(O) 100.4 (μ-ONep) 69.05	90.58

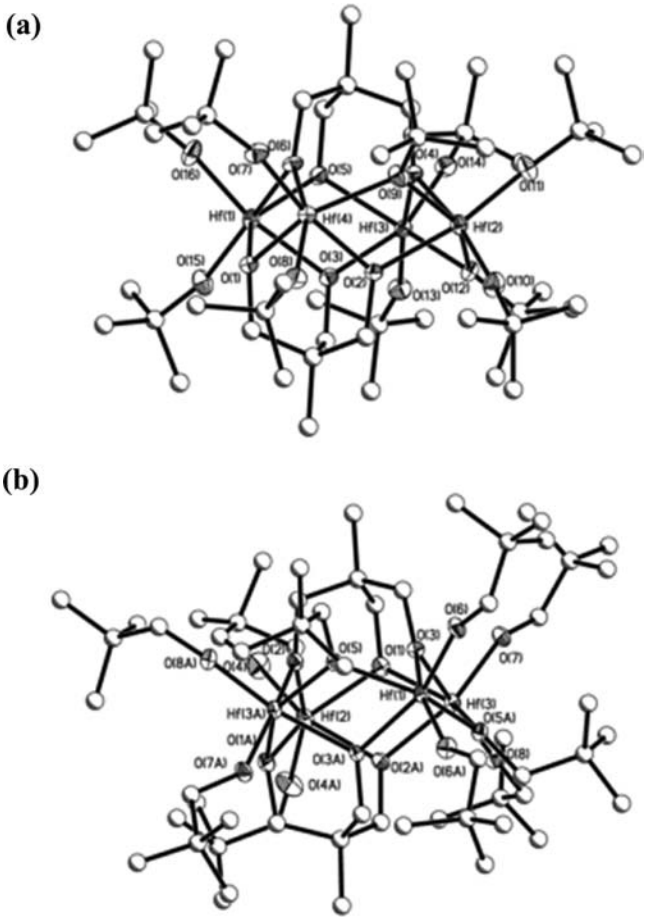

Figure 10. Structure plots of polydentate THME derivatives: (a) **25**; (b) **26**. Thermal ellipsoids of heavy atoms drawn at the 30% level with C atoms drawn as ball and stick for clarity.

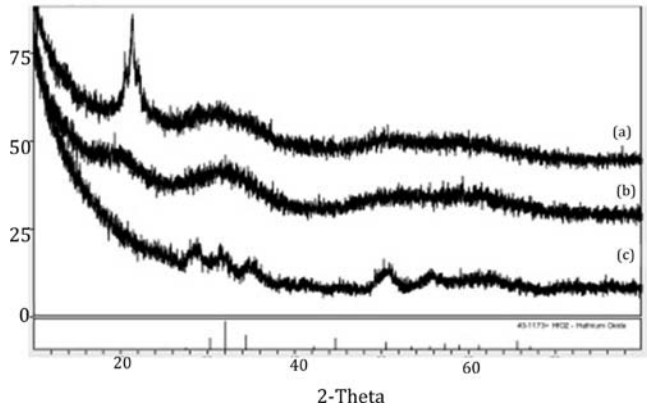

Figure 11. PXRD of nanomaterials generated from **25** (a) as prepared, (b) annealed at125 °C, and (c) annealed at 650 °C in air.

alternative [Hf(OR)$_4$] arrangements. These are discussed below, focusing on a series of solvent-like-substituted methanol derivatives termed HOR* [i.e., H-OTHF (Figure 1h) and H-OPy (Figure 1i)] and the tridentate THME ligands.

*a. HOR**. Previously, the HOR* bidentate ligands were found to form dinuclear and mononuclear titanium compounds,[60] but the impact that the larger Hf metal center would have on the final structure was not known. After the desired HOR* was mixed with [Hf(OBu^t)$_4$], the reaction was stirred for 12 h and then the volatile portion was allowed to slowly evaporate until crystals formed. The FTIR data clearly showed that the OR* ligands had reacted with a number of the OBu^t ligands.

The bidentate OTHF ligand (Figure 1h) was introduced to [Hf(OBu^t)$_4$] in a variety of stoichiometries, but as noted for the titanium system,[60] only the monosubstituted complex was isolated as **22** (Figure 9a). This compound is dinuclear, where each hafnium binds an OTHF ligand that acts as a chelating bridge (μ_c-OTHF) while retaining the original OBu^t ligands. The metrical data for this structure solution are not reliable because of severe disorder in the pendant ligand chains. Elemental analyses were consistent with the observed solid-state structure. The NMR data for **22** present resonances that are broad and varied, with two sharp resonances for OBu^t present in a 1:1 ratio. The breadth of the resonances and two equal OBu^t peaks indicate that either an equilibrium between the monomer and dinuclear structures exists or the THF moiety of the OTHF ligand may bind and unbind, allowing for more variations in the solution structure. The later process is more consistent with what was noted for the titanium system.[60] Variable-temperature NMR data were not pursued because of the preferential crystallization of this compound at even slightly lower temperatures.

The reaction of [Hf(OBu^t)$_4$] with 2 equiv of H-OPy (Figure 1i) led to the dinuclear **23** (Figure 9b); however, the substitution is not symmetrical. The Hf(1) atom possesses three terminal OBu^t ligands and binds to three O atoms of the OPy bridging ligands. Two of these OPy ligands [O(1) and O(2)] chelate bridge [μ_c-OPy] to Hf(2). The remaining OPy O atom[O(3)] is bridging only. The other Hf atom in **23** possesses a terminal OBu^t, a terminal OPy, two μ_c-OPy, and a μ-OPy ligand. This means the first Hf atom adopts a pseudo-OC-6 and the second Hf atom is seven-coordinated. Heating a solution of **23** dissolved in pyridine led to the isolation of **24**, as shown in Figure 9c.

For the two mononuclear molecules per unit cell of **24**, there are two chelating OPy^c ligands and two OBu^t ligands bound to the pseudo-OC-6 Hf metal center. Not surprisingly, the metrical data for **23** and **24** (see Table 6) are very similar to each other and the $(OPy)_2Ti(OR)_2$ derivatives (upon compensation for the change in the cation size).[60] NMR data of **24** dissolved in py-d_5 were consistent with the monomeric species observed in the solid state. The bulk powder elemental analysis was found to be in agreement with the observed crystal structure.

b. THME. Using the tridentate ligand THME (Figure 1j) resulted in the formation of the tetranuclear species **25** and is shown in Figure 10a. The central core of this compound resembles the same structure noted previously for the Zr-THME derivative,[61] where two μ-THME ligands bridge four Hf metal centers. In addition, two μ-OR groups are present and located off of the same Hf metal center. The pseudo-OC-6 metal center is completed through the binding of two terminal OBu^t groups. The metrical data for **25** are in agreement throughout the distances and angles reported and with those of the zirconium derivative.[61] The low solubility of **25** prevented one from obtaining meaningful NMR data; however, elemental analysis of the bulk powder was found to be in agreement with the crystal structure. The THME/ONep derivative **26** (Figure 10b) was also synthesized under conditions similar to those noted for **25** but using $\{[H][(\mu\text{-}ONep)_3Hf_2(ONep)_5(OBu^t)]\}$[35] instead of $[Hf(OBu^t)_4]$. The final product was found to adopt an arrangement and properties identical with those noted for **25**, but for this report, only the structural properties are reported. Metrical data for **25** and **26** are shown in Table 6, and the distances and angles were found to be in agreement with each other and the literature[61] data when the ionic radius is taken into account.

D. Nanoparticle Synthesis. The two methods that have been reported for the production of HfO_2 nanomaterials are sputtering[17−19] and solution[20−22] routes. For solution routes, only the solvothermal (SOLVO) processing of hafnium chloride in the presence of benzyl alcohol[22] led to HfO_2 nanomaterials. The other two efforts focused on making (a) nickel-doped HfO_2[20] from the powder processing of mixed-metal oxide powders in triethanolamine or (b) hafnium oxide@gold (core@shell) nanoparticles[21] using tetrakis(dimethylamino)hafnium processed in the presence of 1,2 hexadecandiol and gold acetate. All three solution routes go through uncharacterized, in situ generated, alkoxide-like intermediates. Therefore, it was of interest to determine the utility of the newly characterized $[Hf(OR)_4]$ precursors (**1**−**26**) in the production of HfO_2 nanomaterials and the impact that their structural arrangements would have on the nanomaterials' final morphology.

The compounds were selected to represent the mononuclear ($[Hf(OBu^t)_4]$ and **8**), dinuclear (**19a** and **22**), and tetranuclear (**25**) species. A SOLVO route using oleylamine/oleic acid as the solvent system was selected because of the propensity of this system to generate nanowires.[62−65] After the reaction had been properly processed, the resulting dark-brown powders were found by PXRD to be amorphous (see Figure 11a). Thermal processing at 125 °C (Figure 11b) did not improve the crystallinity but did remove the organic species noted in the low 2θ range. Final processing at 650 °C in air led to a light-tan material that possessed a broad PXRD pattern that was consistent with crystalline HfO_2 [PDF 00-040-1173 (HfO_2); Figure 11c]. Scherrer equation analyses did not lead to valid particle size determination because of the breadth of the peaks and their variability in the half-height peak width. TEM images (see Figure 12) confirmed that nanomaterials had been successfully synthesized, and EDS analyses

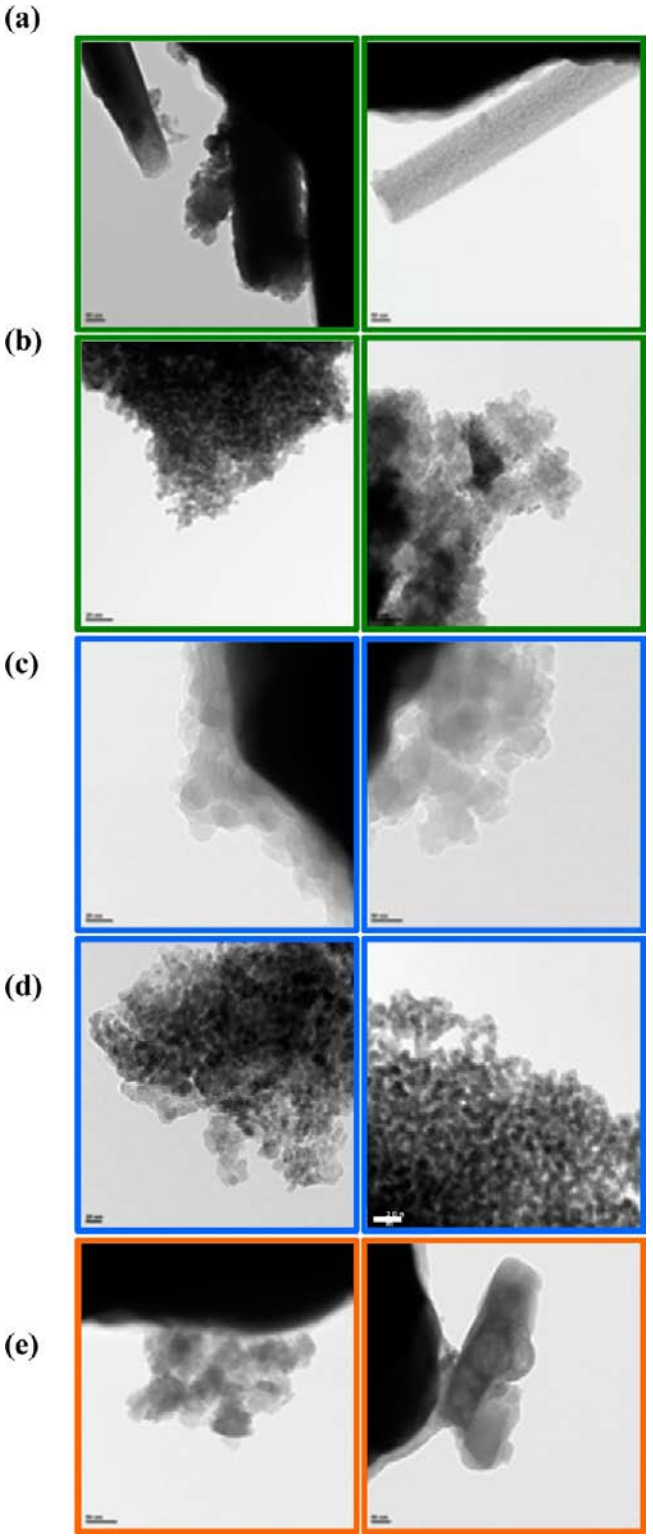

Figure 12. TEM images of nanomaterials generated from (a) $Hf(OBu^t)_4$ (scale bar = 50, 50 nm), (b) **8** [$OC_6H_3(CH_3)_2$-2,6; 20, 50 nm], (c) **19a** [$OC_6H_3(CH(CH_3)_2)_2$-2,6: 20, 50 nm], (d) **22** (OTHF; 20, 20 nm), and (e) **25** (THME; 50, 50 nm) after annealing at 650 °C in air.

revealed the presence of Hf atoms and a trace amount of O atoms with no C atoms (*note*: the weak oxygen peak was attributed to the low signal available because of the sample proximity to the copper grids used). In order to improve the crystallinity of HfO_2, powders from **22** were processed at 1000 °C. The sharper PXRD

dx.doi.org/10.1021/ic300622h | *Inorg. Chem.* 2012, 51, 12075−12092

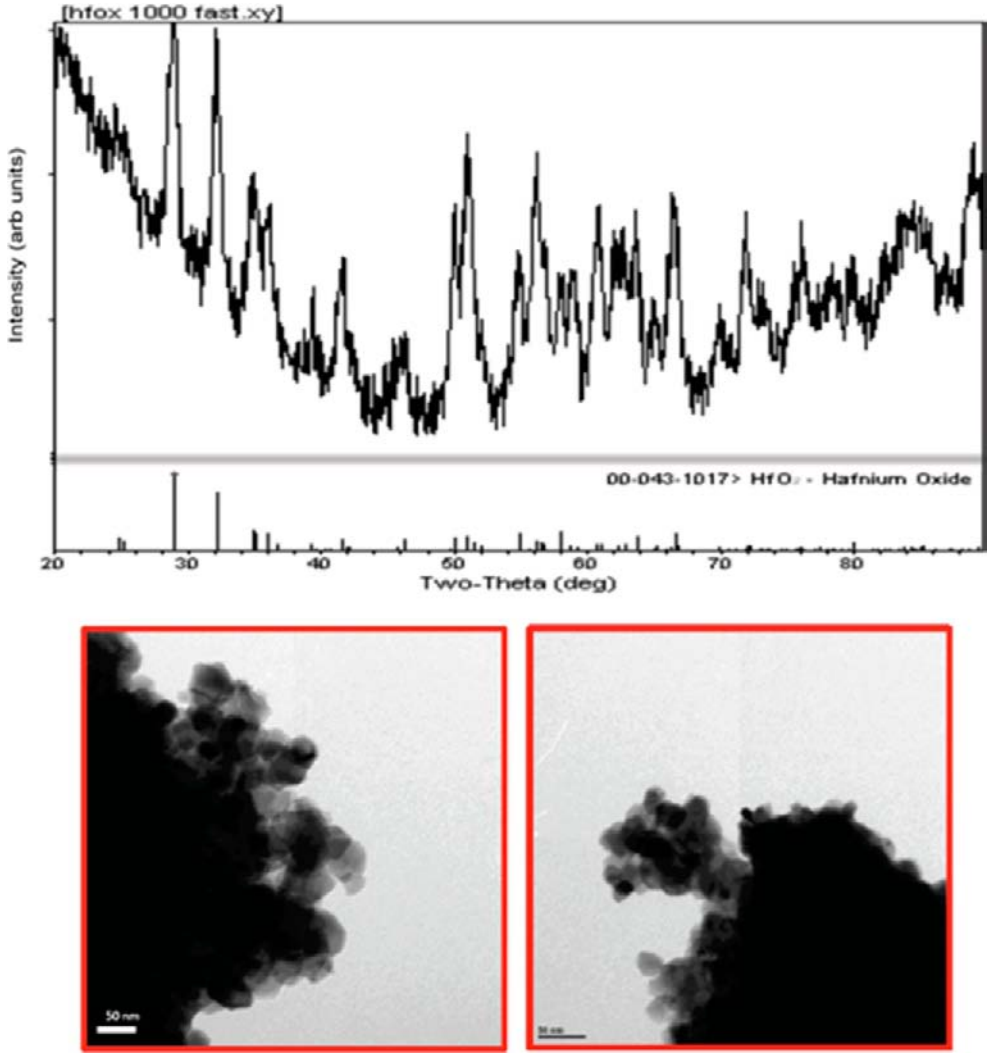

Figure 13. (a) PXRD and (b) TEM images (the scale bar for both is 50 nm) from SOLVO-generated powders from **22** processed at 1000 °C in air.

patterns (see Figure 13a) of the resulting off-white powder were found to be in agreement with HfO_2 (PDF 00-043-1017).[25] TEM images (Figure 13b) revealed that the higher processing temperature had generated some sintering of the particles with sizes now ranging between 20 and 25 nm. EDS analysis was consistent with Hf and O atoms being present as well as a trace amount of C atoms. These data, for the first time, demonstrate the utility of $[Hf(OR)_4]$ precursors for the production of HfO_2 nanomaterials through the SOLVO route discussed.

Previously, we have clearly demonstrated the role that the precursor can play in directing the final morphology of the nanomaterials.[4,9,10] However, the PSA focused on zinc-,[4] germanium-,[9] and cadmium[10]-based ceramic materials. These data allowed us to determine whether the PSA could be employed for tailored HfO_2 nanomaterials. Hafnia reportedly adopt several crystal structures (i.e., monoclinic, cubic, and orthorhombic), which lend themselves to more rodlike structures.[66,67] The initial parent $[Hf(OBu^t)_4]$ precursor was investigated to establish the baseline morphologies that could be obtained under these conditions. On the basis of the monomeric nature of $[Hf(OBu^t)_4]$,[11,36] upon decomposition, the resulting nucleation shower should produce a uniform set of individual growth nuclei and thus produce nanodots. While a variety of different-sized dots ranging in size from 2 to 25 nm were present, a number of unexpected nanorods were observed. These nanorods had an aspect ratio of over 5 (the smallest rod was ~80 nm × 400 nm), but the fine structure of the rods appears to be agglomerated nanoparticles (Figure 12a). In contrast, the other monomeric precursor **8** generated *only* nanodots on the order of 2−4 nm (Figure 12b). For dinuclear species, larger dots or thin rods were expected based on the M_2O_2 central core growth nuclei. As can be observed in Figure 12c, plates ranging from 20 to 30 nm were isolated from **19a**. The other dinuclear precursor **22** yielded only nanodots (10−30 nm; Figure 12d). No rods were noted. Finally, for the tetranuclear precursor **25**, the plane of the Hf_4O_8 central core is capped by the two THME ligands. These growth nuclei should lead to large rod growth or plates. The TEM images revealed large plates on the order of 30−50 nm, as well as a number of rods (Figure 12e). The rods varied in aspect ratios ranging from 4 to >9 (~100 × 900 nm) and appear to have a microstructure that is less granular than that noted for the rods of $[Hf(OBu^t)_4]$. The precursors' growth nuclei and decomposition temperature are speculated to be directed by the various ligand sets. While a great deal more work is necessary to understand, optimize, and verify the PSA for this system, the initial efforts indicate that precursor-induced morphological variations may exist.

dx.doi.org/10.1021/ic300622h | *Inorg. Chem.* 2012, 51, 12075−12092

This lends promise to the design of tailored HfO_2 nanomaterials based on designer $[Hf(OR)_4]$ precursors.

SUMMARY AND CONCLUSION

For the first time, the coordination chemistry of $[Hf(OBu^t)_4]$ was systematically investigated using (i) Lewis basic *solvents*, (ii) simple *phenoxides*, and (iii) *complex polydentate alcohols*. For the Lewis basic solvates, monomeric complexes $[Hf(OBu^t)_4(solv)_n]$ (**1**−**3**) were isolated. The structurally identified OAr products proved to be either $[Hf(OAr)_n(OBu^t)_{4-n}]_2$ (**4** and **5**), $[Hf(\mu\text{-}OH)(OAr)_3(HOBu^t)]_2$ (**6** and **7**), or $[Hf(OAr)_n(OBu^t)_{4-n}(HOBu^t)]$ (**8** and **9**) when toluene is used as the solvent or solvated monomeric compounds $[Hf(OAr)_n(OBu^t)_{4-n}(solv)_x]$ (**10**−**21**) when Lewis basic solvents are used. The majority of these compounds (**4**−**21**) were found to have Hf metal centers that adopt either a distorted five-coordinate (SBP or TBP, with the former being the preferred mode) or a six-coordinate (pseudo-OC-6) geometry. In several instances, a retained OBu^t was identified as a coordinated $HOBu^t$ (**4** and **6**−**9**) versus a solvated HOAr complex; however, a bound HOR was not found for any of the crystals that employed a Lewis basic solvent. The steric bulk of $OC_6H_3\text{-}(C(CH_3)_3)_2$-2,6 and OBu^t only allowed for one ligand exchange, as noted for **9**, **15**, and **21**. Interestingly, for the $OC_6H_4\text{-}(C(CH_3)_3)$-2 systems investigated, only oils were isolated unless an oxo species (**6**) formed. Oxo formation was noted for long-term crystal growth of the toluene species, yielding dinuclear complexes with OH bridging ligands (**4a**, **5a**, **6**, and **7**). The oxo formation occurred only for the less sterically hindered OAr derivatives; however, this might be due to their longer crystallization time and thus greater chance of potential exposure to adventitious oxygen or water versus the shorter, quicker crystal growth of the larger OAr species (**8** and **9**). Additionally, **19a** showed that, even for Lewis basic solvents, oxo formation was possible. Polydentate ligands were found to generate more complex precursors (**22**−**26**), but the final structures are similar to the smaller titanium congener species previously isolated. The low nuclearity observed in this study is believed to be due to the steric bulk of OBu^t, so additional studies that use the less sterically demanding OEt (i.e., $[Hf(OEt)_4]$) and polydentate ligands are underway to elicit more complex precursor types. SOLVO processing of select, structurally varied alkoxide precursors (monomer, $[Hf(OBu^t)_4]$ and **8**; dimer, **19a** and **22**; tetramer, **25**) were evaluated for the production of HfO_2 nanomaterials under identical processing conditions. The resulting products were found to generate HfO_2 dots, plates, and rods, indicating that the precursors may have an impact on the final morphology. Additional work to exploit the PSA to obtain designed HfO_2 nanomaterial morphologies is underway.

AUTHOR INFORMATION

Corresponding Author

*E-mail: tjboyle@Sandia.gov. Phone: (505)272-7625. Fax: (505) 272-7336.

Notes

The authors declare no competing financial interest.

ACKNOWLEDGMENTS

The authors thank the National Institute for Nanoengineering and Laboratory Directed Research and Development programs at Sandia National Laboratories for support of this work and are grateful for use of the Bruker X-ray diffractometer purchased via the National Science Foundation CRIF:MU award to Professor Kemp of the University of New Mexico (Grant CHE04-43580). Sandia National Laboratories is a multiprogram laboratory managed and operated by Sandia Corp., a wholly owned subsidiary of Lockheed Martin Corp., for the U.S. Department of Energy's National Nuclear Security Administration under Contract DE-AC04-94AL85000.

REFERENCES

(1) Boyle, T. J.; Tribby, L. J.; Ottley, L. A. M.; San, S. M. *Eur. J. Inorg. Chem.* **2009**, *36*, 5550.
(2) Hernandez-Sanchez, B. A.; Boyle, T. J.; Pratt, H. D. I.; Rodriguez, M. A.; Brewer, L. N.; Dunphy, D. R. *Chem. Mater.* **2008**, *20*, 6643.
(3) Boyle, T. J.; Hernandez-Sanchez, B. A.; Baros, C. M.; Brewer, L. N.; Rodriguez, M. A. *Chem. Mater.* **2007**, *19*, 2016.
(4) Boyle, T. J.; Bunge, S. D.; Andrews, N. L.; Matzen, L. E.; Sieg, K.; Rodriguez, M. A.; Headley, T. J. *Chem. Mater.* **2004**, *16*, 3279.
(5) Caulton, K. G.; Hubert-Pfalzgraf, L. G. *Chem. Rev.* **1990**, *90*, 969.
(6) Chandler, C. D.; Roger, C.; Hampden-Smith, M. J. *Chem. Rev.* **1993**, *93*, 1205.
(7) Hubert-Pfalzgraf, L. G. *New J. Chem.* **1987**, *11*, 663.
(8) Turova, M. Y.; Turevskaya, E. P.; Kessler, V. G.; Yanovskaya, M. I. *The Chemistry of Metal Alkoxides*; Kluwer Academic Publishers: Boston, 2002.
(9) Gerung, H.; Boyle, T. J.; Tribby, L. J.; Bunge, S. D.; Brinker, C. J.; Han, S. M. *J. Am. Chem. Soc.* **2006**, *128*, 5244.
(10) Boyle, T. J.; Bunge, S. D.; Alam, T. M.; Holland, G. P.; Headley, T. J.; Avilucea, G. *Inorg. Chem.* **2005**, *44*, 1309.
(11) Bradley, D. C.; Mehrotra, R. C.; Rothwell, I. P.; Singh, A. *Alkoxo and Aryloxo Derivatives of Metals*; Academic Press: San Diego, 2001.
(12) *Conquest*, version 1.13; Cambridge Crystallographic Data Centre: Cambridge, U.K.; support@ccdc.cam.ac.uk or http://www.ccdc.cam.ac.uk [CSD version 5.32 (November 2010)].
(13) Imam, S. A.; Rao, B. R. *Naturwissenschaften* **1963**, *50*, 517.
(14) Veith, M.; Mathur, S.; Mathur, C.; Huch, V. *J. Chem. Soc., Dalton Trans.* **1997**, 2101.
(15) Williams, P. A.; Roberts, J. L.; Jones, A. C.; Chalker, P. R.; Bickley, J. F.; Steiner, A.; Davies, H. O.; Leedham, T. J. *J. Mater. Chem.* **2002**, *12*, 165.
(16) Williams, P. A.; Roberts, J. L.; Jones, A. C.; Chalker, P. R.; Tobin, N. L.; Bickley, J. F.; Davies, H. O.; Smith, L. M.; Leedham, T. J. *Chem. Vap. Dep.* **2002**, *8*, 163.
(17) Li, H.-M.; Zhang, G.; Yang, C.; Lee, D.-Y.; Lim, Y.-D.; Shen, T.-Z.; Yoo, W. J.; Park, Y. J.; Kim, H.; Cha, S. N.; Kim, J. M. *J. Appl. Phys.* **2011**, *109*, 093516(1/8).
(18) Verrelli, E.; Tsoukala, D. *Microelectron. Eng.* **2011**, *88*, 1189.
(19) Qiu, X.; Howe, J. Y.; Cardoso, M. B.; Polat, O.; Heller, W. T.; Paranthaman, M. P. *Nanotechnology* **2009**, 455601(1/9).
(20) Sharma, M. K.; Mishra, D. K.; Ghosh, S.; Kanjilal, D.; Srivastava, P.; Chatterjee, R. *J. Appl. Phys.* **2011**, *110*, 063902.
(21) Dahal, N.; Chikan, V. *Inorg. Chem.* **2012**, *51*, 518.
(22) Buha, J.; Arcon, D.; Niederberger, M.; Djerdj, I. *Phys. Chem. Chem. Phys.* **2010**, 15537.
(23) Boyle, T. J.; AlShareef, H. N. *J. Mater. Sci.* **1997**, *32*, 2263.
(24) Weiss, E.; Alsdorf, H.; Kuhr, H. *Angew. Chem., Int. Ed.* **1967**, *79*, 801.
(25) *XRD Pattern Processing*; Jade, Inc.: Mission Hills, CA, 1999.
(26) Viljoen, J. A.; Visser, H. G.; Roodt, A.; Steyn, M. *Acta Crystallogr., Sect E: Struct. Rep. Online* **2009**, *65*, m1514.
(27) Viljoen, J. A.; Visser, H. G.; Roodt, A. *Acta Crystallogr., Sect E: Struct. Rep. Online* **2010**, *66*, m603.
(28) Blackmore, K. J.; Sly, M. B.; Haneline, M. R.; Ziller, J. W.; Heyduk, A. F. *Inorg. Chem.* **2008**, *47*, 10522.
(29) Chmura, A. J.; Davidson, M. G.; Jones, M. D.; Lunn, M. D.; Mahon, M. F. *Dalton Trans.* **2006**, 887.
(30) Chmura, A. J.; Davidson, M. G.; Jones, M. D.; Lunn, M. D.; Mahon, M. F.; Johnson, A. J.; Khunkamchoo, P.; Roberts, S. L.; Wong, S. S. F. *Macromolecules* **2006**, *39*, 7250.

(31) Loo, Y. F.; O'Kane, R.; Jones, A. C.; Aspinall, H. C.; Potter, R. J.; Chalker, P. R.; Bickley, J. F.; Taylor, S.; Smith, L. M. *J. Mater. Chem.* **2005**, *15*, 1896.
(32) Boyle, T. J.; Pratt, H. D.; Ottley, L. A. M.; Alam, T. M.; McIntyre, S. K.; Rodriguez, M. A.; Farrell, J.; Campana, C. F. *Inorg. Chem.* **2009**, *48*, 9191.
(33) Starikova, Z. A.; Turevskaya, E. P.; Kozlova, N. I.; Turova, N. Y.; Berdyev, D. V.; Yanovsky, A. I. *Polyhedron* **1999**, *18*, 941.
(34) Boyle, T. J.; Tribby, L. J.; Alam, T. M.; Bunge, S. D.; Holland, G. P. *Polyhedron* **2005**, *24*, 1143.
(35) Boyle, T. J.; Ottley, L. A. M.; Hoppe, S. M. *Inorg. Chem.* **2010**, *49*, 10798.
(36) Shannon, R. D. *Acta Crystallogr.* **1976**, *A32*, 751.
(37) Terry, K. W.; Lugmair, C. G.; Tilley, T. D. *J. Am. Chem. Soc.* **1997**, *119*, 9745.
(38) Lugmair, C. G.; Tilley, T. D. *Inorg. Chem.* **1998**, *37*, 764.
(39) Milanov, A.; Bhakta, R.; Thomas, R.; Ehrhart, P.; Winter, M.; Waser, R.; Devi, A. *J. Mater. Chem.* **2006**, *16*, 437.
(40) Roberts, J. L.; Marshall, P. A.; Jones, A. C.; Chlaker, P. R.; Bickley, J. F.; Williams, P. A.; Taylor, S.; Smith, L. M.; Critchlow, G. W.; Schumacher, M.; Lindner, J. *J. Mater. Chem.* **2004**, *14*, 391.41. Bradley, D. C.; Mehrotra, R. C.; Gaur, D. P. *Metal Alkoxides*; Academic Press: London, 1978.
(41) Bradley, D. C.; Mehrotra, R. C.; Gaur, D. P. *Metal Alkoxides.* Academic Press: London, 1978.
(42) Boyle, T. J.; Schwartz, R. W.; Doedens, R. J.; Ziller, J. W. *Inorg. Chem.* **1995**, *34*, 1110.
(43) Vaartstra, B. A.; Huffman, J. C.; Gradeff, P. S.; Hubert-Pfalzgraf, L. G.; Daran, J.-C.; Parraud, S.; Yunlu, K.; Caulton, K. G. *Inorg. Chem.* **1990**, *29*, 3126.
(44) Kobayashi, S.; Yazaki, R.; Seki, K.; Ueno, M. *Tetrahedron* **2007**, *63*, 8425.
(45) Boyle, T. J.; Tribby, L. J.; Alam, T. M.; Bunge, S. D.; Holland, G. P. *Polyhedron* **2005**, *24*, 1143.
(46) Spijksma, G. I.; Bouwmeester, H. J. M.; Blank, D. H. A.; Fischer, A.; Henry, M.; Kessler, V. G. *Inorg. Chem.* **2006**, *45*, 4938.
(47) Viljoen, J. A.; Visser, H. G.; Roodt, A.; Steyn, M. *Acta Crystallogr., Sect E: Struct. Rep. Online* **2009**, *65*, m1367.
(48) Morozova, N. B.; Zherikova, K. V.; Badina, I. A.; Sysoev, S. V.; Glenfold, N. V.; Igumenov, I. K. *Monogr. Ser. Int. Conf. Coord. Chem.* **2005**, *7*, 246.
(49) Zherikova, K. V.; Morozova, N. B.; Baidina, I. A.; Alekseev, V. I.; Igumenov, I. K. *Zh. Strukt. Khim.* **2006**, *47*, 87.
(50) Dalgarno, S. J.; Atwood, J. L.; Raston, C. L. *Inorg. Chim. Acta* **2007**, *360*, 1344.
(51) Fanccini, F.; Fric, H.; Schubert, U.; Wendel, E.; Tsetsgee, O.; Muller, K.; Bertagnolli, H.; Venso, A.; Gross, S. *J. Mater. Chem.* **2007**, *17*, 3297.
(52) Mit'kina, T. V.; Geras'ko, O. A.; Sokolov, M. N.; Naumov, D. Y.; Fedin, V. P. *Izv. Akad. Nauk SSR, Ser. Khim. (Russ. Chem. Bull.)* **2004**, 80.
(53) Nomiya, K.; Saku, Y.; Yamada, S.; Takahashi, W.; Sekiya, H.; Shinohara, A.; Ishimaru, M.; Sakai, Y. *Dalton Trans.* **2009**, 5504.
(54) Otero, A.; Fernandez-Baeza, J.; Antinolo, A.; Tejeda, J.; Lara-Sanchez, A.; Sanchez-Barba, L.; Fernandez-Lopez, M.; Lopez-Solera, I. *Inorg. Chem.* **2004**, *43*, 1350.
(55) Addison, A. W.; Nageswara, R.; Reedijk, J.; van Rijn, J.; Verschoor, G. C. *J. Chem. Soc., Dalton Trans.* **1984**, 1349.
(56) Puchberger, M.; Kogler, F. R.; Jupa, M.; Gorss, S.; Fric, H.; Kickelbick, G.; Schubert, U. *Eur. J. Inorg. Chem.* **2006**, 3283.
(57) Qiu, R.; Zhang, G.; Zhu, Y.; Xu, X.; Shao, L.; Li, Y.; An, D.; Yin, S. *Chem.—Eur. J.* **2009**, *15*, 6488.
(58) Ryu, S.; Kim, J.; Yeo, H.; Kim, K. *Inorg. Chim. Acta* **1995**, *228*, 233.
(59) http://www.chemicalize.org.
(60) Boyle, T. J.; Sewell, R. M.; Ottley, L. A. M.; Pratt, H. D.; Quintana, C. J.; Bunge, S. D. *Inorg. Chem.* **2007**, *46*, 1825.
(61) Boyle, T. J.; Schwartz, R. W.; Doedens, R. J.; Ziller, J. W. *Inorg. Chem.* **1995**, *34*, 1110.
(62) Xiaoping, J.; Kruszynska, M.; Parisi, J.; Kolny-Olesiak, J. *Nano Res.* **2011**, *4*, 824.
(63) Peng, Z. M.; You, H. J.; Yang, H. *ACS Nano* **2010**, *4*, 1501.
(64) Choi, S. H.; Kim, E. G.; Park, J.; An, K.; Lee, N.; Kim, S. C.; Hyeon, T. *J. Phys. Chem. B* **2005**, *109*, 14792.
(65) Cha, S. I.; Mo, C. B.; Kim, K. T.; Hong, S. H. *J. Mater. Res.* **2005**, *20*, 2148.
(66) Perevalov, T. V.; Gritsenko, V. A.; Erenburg, S. B.; Badalyan, A. M.; Wong, H. *J. Appl. Phys.* **2007**, *101*, 053704.
(67) Ruh, R.; Corfield, P. W. R. *J. Am. Ceram. Soc.* **1970**, 126.